

1 Cosmogenic ages indicate no MIS 2 refugia in the Alexander 2 Archipelago, Alaska

3
4 Caleb K. Walcott¹, Jason P. Briner¹, James F. Baichtal², Alia J. Lesnek³, Joseph M. Licciardi⁴

5 ¹Department of Geology, University at Buffalo, Buffalo, NY 14260, USA

6 ²Tongass National Forest, Thorne Bay, AK 99919, USA

7 ³School of Earth and Environmental Sciences, CUNY Queens College, Flushing, NY 11367,
8 USA

9 ⁴Department of Earth Sciences, University of New Hampshire, Durham, NH 03824, USA

10 *Correspondence to:* Caleb K. Walcott (ckwalcot@buffalo.edu)

11 **Abstract**

12
13 The late-Pleistocene history of the coastal Cordilleran Ice Sheet remains relatively unstudied
14 compared to chronologies of the Laurentide Ice Sheet. Yet accurate reconstructions of
15 [Cordilleran Ice Sheet](#) extent and [the](#) timing of ice retreat along the Pacific Coast are essential for,
16 paleoclimate modeling, assessing meltwater contribution to the North Pacific, and determining
17 the availability of ice-free land along the coastal [Cordilleran Ice Sheet](#) margin for human
18 migration from Beringia into the [rest of the](#) Americas. To improve the chronology of [Cordilleran](#)
19 [Ice Sheet](#) history in the Alexander Archipelago, Alaska, we applied ¹⁰Be and ³⁶Cl dating to
20 boulders and glacially sculpted bedrock in areas previously hypothesized to have remained ice-
21 free throughout the local Last Glacial Maximum ([LLGM](#); 20-17 ka). Results indicate that these
22 sites, and more generally the coastal northern Alexander Archipelago, became ice-free by 15.1 ±
23 0.9 ka (n = 12 boulders; 1 SD). We also provide further age constraints on deglaciation along the
24 southern Alexander Archipelago and combine our new ages with data from two previous studies.
25 We determine that ice retreated from the outer coast of the southern Alexander Archipelago at
26 16.3 ± 0.8 ka (n = 14 boulders; 1 SD). These results collectively indicate that areas above

Formatted: Default Paragraph Font, Font: +Body (Calibri), Font color: Black

Formatted: Default Paragraph Font, Font: +Body (Calibri), Font color: Black

Formatted: Normal, Right, Border: Top: (No border), Bottom: (No border), Left: (No border), Right: (No border), Between : (No border), Tab stops: 3.25", Centered + 6.5", Right, Position: Horizontal: Left, Relative to: Column, Vertical: In line, Relative to: Margin, Wrap Around

Formatted: Font: Calibri, Font color: Black

Deleted: A cosmogenic nuclide chronology of Cordilleran Ice Sheet configuration during the Last Glacial Maximum in the northern

Formatted

Formatted: Font: 15.5 pt, Font color: Custom Color(70,70,70)

Formatted: Font: 21 pt

Formatted: Line spacing: Multiple 1.15 li

Deleted: (CIS)

Deleted: CIS

Deleted: a variety of reasons including

Deleted: CIS

Deleted: CIS

Deleted: outcrops

Deleted: ILGM

2

Formatted: Default Paragraph Font, Font: +Body (Calibri), Font color: Black

Formatted: Default Paragraph Font, Font: +Body (Calibri), Font color: Black

Formatted: Normal, Right, Border: Top: (No border), Bottom: (No border), Left: (No border), Right: (No border), Between : (No border), Tab stops: 3.25", Centered + 6.5", Right, Position: Horizontal: Left, Relative to: Column, Vertical: In line, Relative to: Margin, Wrap Around

Formatted: Font: Calibri, Font color: Black

Deleted: ILGM

Deleted: ILGM

Deleted: CIS

Formatted: Space Before: 0 pt, After: 0 pt

37 modern sea level that were previously mapped as glacial refugia were covered by ice during the
38 LLGM until between ~16.3 and 15.1 ka. As no evidence was found for ice-free land during the
39 LLGM, our results suggest that previous ice-sheet reconstructions underestimate the regional
40 maximum Cordilleran Ice Sheet extent, and that all ice likely terminated on the continental shelf.
41 Future work should investigate whether presently submerged areas of the continental shelf were
42 ice-free.

44 1 Introduction

45 The late-Pleistocene history of the coastal Cordilleran Ice Sheet remains relatively unstudied
46 compared to chronologies of the Laurentide Ice Sheet (Dalton et al., 2020). Cordilleran Ice
47 Sheet margin reconstructions from the Pacific Coast are based largely on qualitative field
48 observations with little chronologic control (Dyke, 2004; Carrara et al., 2007; Dalton et al.,
49 2020). While a few studies have recently generated local ice sheet retreat chronologies from
50 terrestrial locations along the Pacific Coast (Darvill et al., 2018; Lesnek et al., 2018; Lesnek et
51 al., 2020), there are still large areas of the southeastern Alaskan coastline that lack direct age
52 constraints on deglaciation (Fig. 1). Much of the Northern Hemisphere was covered by
53 continental ice sheets during the global Last Glacial Maximum (GLGM; ~26 – 19 ka).
54 Chronologies of northern hemisphere glaciation have revealed that while the Laurentide Ice
55 Sheet and many alpine glaciers worldwide were at their greatest extents during the global Last
56 Glacial Maximum (GLGM; ~26-19 ka), the coastal Cordilleran Ice Sheet and the Puget Lobe
57 reached their maximum size ~20 – 17 cal ka (local Last Glacial Maximum; hereafter LLGM ;
58 Porter and Swanson, 1998; Booth et al., 2003; Praetorius and Mix, 2014; Darvill et al., 2018;
59 Lesnek et al., 2018). Other studies have also explored the Cordilleran Ice Sheet contributions to

Deleted: →

Formatted: Indent: First line: 0"

Deleted: (CIS)

Deleted: (LIS;

Deleted: CIS

Deleted:),

Deleted: remain vast stretches

Deleted: Pacific

Formatted: Font: +Body (Calibri), 11 pt

Deleted:

Deleted: Accurate reconstructions of CIS extent and the timing of ice retreat along the Pacific Coast are essential for paleoclimate modeling, assessing glacial meltwater contributions to the North Pacific and subsequent Northern Hemisphere climate impacts, predicting future mass loss from other marine-terminating ice sheets, and determining whether a coastal route from Beringia into the Americas was viable for humans during southward migration. ¶

Deleted: gLGM

Deleted: While

Deleted: LIS

Deleted: this time,

Deleted: CIS

Deleted: ILGM

Deleted: ¶
Accurate constraints of CIS deglaciation are necessary to investigate research topics across numerous disciplines. Recent...

Deleted: CIS

3

Formatted: Default Paragraph Font, Font: +Body (Calibri), Font color: Black

Formatted: Normal, Right, Border: Top: (No border), Bottom: (No border), Left: (No border), Right: (No border), Between : (No border), Tab stops: 3.25", Centered + 6.5", Right, Position: Horizontal: Left, Relative to: Column, Vertical: In line, Relative to: Margin, Wrap Around

Formatted: Default Paragraph Font, Font: +Body (Calibri), Font color: Black

Formatted: Font: Calibri, Font color: Black

Deleted: LIS

Deleted: CIS

Deleted: CIS

Deleted: CIS

Deleted: had

Deleted: CIS

Deleted: CIS

Deleted: CIS

Deleted: throughout

Deleted: ILGM.

Deleted: CIS

Deleted: to

Deleted: CIS

Deleted: (SE AK),

Deleted: to

Deleted: ILGM

Deleted: from

Deleted: CIS

Deleted: the

Deleted: northern Alexander Archipelago

Deleted: CIS

Deleted: while expanding

90 meltwater pulse 1A (~14.6 ka) following the saddle collapse between the [Laurentide Ice Sheet](#)

91 and [Cordilleran Ice Sheet](#) (Gregoire et al., 2016; Ivanovic et al., 2017). Improved constraints on

92 [Cordilleran Ice Sheet](#) history around [the time of](#) meltwater pulse 1A are necessary to elucidate

93 any influences [of](#) coastal [Cordilleran Ice Sheet](#) configuration and retreat [on](#) saddle collapse.

94 Additionally, numerical modeling studies show differing responses of the [Cordilleran Ice Sheet](#)

95 to last deglacial climate oscillations, thus highlighting the need for an improved [Cordilleran Ice](#)

96 [Sheet](#) chronology to bolster model improvement and validation (Tarasov et al., 2012; Seguinot et

97 al., 2014; Gregoire et al., 2016; Seguinot et al., 2016; Ivanovic et al., 2017). Finally, a temporally

98 accurate paleogeographic reconstruction of the coastal [Cordilleran Ice Sheet](#) margin is required

99 to assess whether a viable coastal route existed for early Americans migrating from Beringia into

100 the Americas. This route hinges on the presence of ice-free land (refugia) suitable for human

101 habitation [during](#) the [migration event\(s\)](#). Earlier mapping efforts and other supporting

102 information indicate areas of potential refugia along the former coastal [Cordilleran Ice Sheet](#)

103 margin (Demboski et al., 1999; Cook et al., 2001; Carrara et al., 2003; Carrara et al., 2007;

104 Shafer et al., 2010; Shafer et al., 2011; [Hebda et al., 2022](#)).

105 This study has two goals: 1) [improve](#) the spatio-temporal patterns of coastal [Cordilleran](#)

106 [Ice Sheet](#) deglaciation in southeastern Alaska [and](#) 2) [assess](#) whether areas of the northern

107 Alexander Archipelago mapped as refugia were ice-free throughout the [LLGM](#) [and](#) thus

108 available for human habitation (Fig. 2). We report 25 new cosmogenic ¹⁰Be exposure ages from

109 boulders and bedrock [in](#) the northern Alexander Archipelago – the first exposure ages

110 documenting [Cordilleran Ice Sheet](#) retreat from [this](#) coastal [region](#). We also report four ¹⁰Be and

111 four cosmogenic ³⁶Cl ages from Suemez Island in the southern Alexander Archipelago. Our data

112 constrain the deglaciation of the marine-terminating [Cordilleran Ice Sheet](#) margin [and](#) [expand](#) the

135 overall North Pacific coastal glacial chronology. Our results suggest deglaciation of coastal
136 regions ~15.4 – 14.8 ka in the northern Alexander Archipelago and do not support previous
137 mapping of refugia in areas that are presently above sea level.

4

Formatted: Normal, Right, Border: Top: (No border), Bottom: (No border), Left: (No border), Right: (No border), Between: (No border), Tab stops: 3.25", Centered + 6.5", Right, Position: Horizontal: Left, Relative to: Column, Vertical: In line, Relative to: Margin, Wrap Around

Formatted: Default Paragraph Font, Font: +Body (Calibri), Font color: Black

Formatted: Default Paragraph Font, Font: +Body (Calibri), Font color: Black

Formatted: Font: Calibri, Font color: Black

Deleted: that shows

139 2 Setting

140
141 The Alexander Archipelago, [southeast Alaska](#), stretches ~480 km (Fig. 2) along the
142 western coast of British Columbia. The southern part of the archipelago is dominated by Prince
143 of Wales Island and surrounding islands, whereas the northern part encompasses Baranof and
144 Chichagof Islands and a collection of smaller islands. The Alexander Archipelago consists of
145 accreted terranes ([Triassic to Cretaceous](#), in age) with quartz-bearing diorite and granodiorite
146 units and notable Eocene-Miocene granitic intrusive complexes (Wilson et al., 2015). Late-
147 Pleistocene volcanic activity on southern Kruzof Island formed the Mt. Edgumbe volcanic
148 field (Riehle, 1996). Post-[LLGM](#) (late-Pleistocene and Holocene) eruptions formed extensive
149 andesite flows on the island and blanketed much of the surrounding area with tephra (Riehle et
150 al., 1984; Riehle et al., 1992; Riehle, 1996). Modern climate of the Alexander Archipelago is
151 dominated by cool, wet summers and mild winters, with perennial heavy rainfall - [Sitka \(Baranof
152 Island\) receives ~2200 mm/yr while Chichagof Island receives over 3300 mm/yr \(Ager, 2019;
153 <https://wrcc.dri.edu/summary/Climsmak.html>\)](#). Snowfall is minimal at lower elevations, but
154 more substantial in higher elevation areas (<https://wrcc.dri.edu/summary/Climsmak.html>).
155 Glaciers occupy alpine cirques in the Alexander Archipelago (totaling < 150 km²), primarily on
156 Baranof and Chichagof islands (Molnia, 2008). Presently, low-elevation (< 700 m asl) areas of

Deleted: SE AK

Deleted: to Triassic

Deleted: ILGM

Deleted: (Ager, 2019).

162 the archipelago are dominated by coniferous [rainforests](#), while alpine tundra exists above the tree
163 line (> 700 m asl; Ager, 2019).

164 Previous mapping shows much, if not all, of [southeast Alaska](#) covered by the [Cordilleran](#)
165 [Ice Sheet](#) during the [LLGM](#) and the last deglaciation, with a maximum position likely
166 terminating several kilometers out on the continental shelf of the Gulf of Alaska (Carrara et al.,
167 2007). Ice caps formed atop the Coast Mountains and high massifs of the Alexander Archipelago,
168 coalesced and flowed westward to the continental shelf and the Pacific Ocean (Capps, 1932;
169 Mann, 1986; Mann and Hamilton, 1995). Outlet glaciers occupied the present fjord and strait
170 landscape (Carrara et al., 2007). Today, the landscape is strewn with clear indicators of
171 widespread glaciation [including](#) deep fjords, glacially sculpted bedrock draped with boulders,
172 and a variety of other glacial landforms, but it remains unclear whether all of [southeast Alaska](#)
173 was covered by the [Cordilleran Ice Sheet](#) during the [LLGM](#). Some areas of the Alexander
174 Archipelago, presently above sea level, [are hypothesized to have been](#) ice-free throughout the
175 [LLGM](#) (Carrara et al., 2007). Recent studies using ¹⁰Be surface exposure dating of glacial
176 landforms, however, indicate that some of these [purported](#) ice-age refugia in the southern
177 Alexander Archipelago were covered by the [Cordilleran Ice Sheet](#) during its [LLGM](#) advance
178 (Lesnek et al., 2018). Other areas previously [mapped](#) as ice age refugia in the northern Alexander
179 Archipelago (Carrara et al., 2007; Dalton et al., 2020) [are investigated in this study; if their](#)
180 [presence is](#) confirmed with numerical dating techniques, this would be a significant confirmation
181 of the existence of coastal refugia.

183 3 Methods

184

5

Formatted: Default Paragraph Font, Font: +Body (Calibri), Font color: Black

Formatted: Default Paragraph Font, Font: +Body (Calibri), Font color: Black

Formatted: Normal, Right, Border: Top: (No border), Bottom: (No border), Left: (No border), Right: (No border), Between: (No border), Tab stops: 3.25", Centered + 6.5", Right, Position: Horizontal: Left, Relative to: Column, Vertical: In line, Relative to: Margin, Wrap Around

Formatted: Font: Calibri, Font color: Black

Deleted: rain forests

Formatted: Indent: First line: 0", Space After: 0 pt

Deleted: SE AK

Deleted: CIS

Deleted: ILGM

Deleted: ,

Deleted: ,

Deleted: (

Deleted:),

Deleted: SE AK

Deleted: CIS

Deleted: ILGM

Deleted: were mapped as

Deleted: ILGM

Deleted: areas of hypothesized

Deleted: CIS

Deleted: ILGM

Deleted: interpreted

Deleted: are investigated in this study.¶
Knowledge of the late-Pleistocene glacial history of the southern Alexander Archipelago and areas of coastal British Columbia has recently improved. Radiocarbon-dated marine sediments indicate that the CIS reached its maximum extent sometime between ~25 and ~18 ka in SE AK (Mann and Hamilton, 1995; Barrie and Conway, 1999; Praetorius and Mix, 2014). Later work, combining ¹⁴C dating of terrestrial macrofossils from Shuká Káa and ¹⁰Be dating of glacial erratics and sculpted bedrock demonstrated maximum CIS extent in the Prince of Wales Island region between ~19.8 and ~17 ka, followed by rapid retreat between ~17 and 15 ka, leading to ice-free inner fjords and sounds by 15 ka and a transition to a primarily land-terminating ice sheet thereafter (Lesnek et al., 2018; Lesnek et al., 2020; Baichtal et al., in press). A speleothem from Prince of Wales records a growth hiatus from 41.5 ± 0.2 ka to 13.4 ± 0.2 ka, interpreted as the presence of permafrost and/or the CIS over the cave, and thus mean annual air temperatures below 0°C during this time (Wilcox et al., 2019). About 400 km to the south (... [1])

Deleted: shows ice-free coastal terrain currently above sea level during the ILGM

272 **3.1 Boulder and bedrock sampling**

273
274 We collected 29 samples (11 bedrock, 18 boulder) for cosmogenic ¹⁰Be surface exposure
275 dating (hereafter ¹⁰Be dating) during summer 2018, 2019, and 2020 (Figs. 3 and 4) from several
276 sites in coastal Southeast Alaska, including Suemez (n = 4), Baranof (n = 11), Biorca (n = 4),
277 Kruzof (n = 4) and Chichagof (n = 6) islands. Our samples range in elevation from ~50 to ~930
278 m asl; all sites are above the local marine limits of ~10 – 20 m asl (Baichtal et al., 2021). We
279 preferentially sampled paired sites consisting of stable boulders and neighboring unvegetated
280 bedrock surfaces. This strategy allowed us to assess whether bedrock surfaces contain isotopic
281 inheritance, and provides insights into ice-sheet erosion history. In the absence of suitable
282 boulders at a few locations, we sampled bedrock with clear evidence of glacial erosion to
283 mitigate the possibility of ¹⁰Be inheritance.

284 We also collected samples from four glacially-transported boulders on the southwestern
285 portion of Suemez Island for ³⁶Cl surface exposure dating during the summer 2019 field season
286 (Figs. 5; 6; Table 2). The boulders consist of non-vesicular olivine basalt of “Tertiary to
287 Quaternary” age (Eberlein et al., 1983).

288 Surface samples were collected from the upper few centimeters of the boulders and
289 bedrock using a handheld angle grinder, hammer, and chisel. We avoided sampling areas of the
290 boulder tops and bedrock surfaces with visible signs of surface erosion (e.g., fractures,
291 weathering pits). We did, however, observe erosional features on the boulders sampled for ³⁶Cl
292 dating. We avoided collecting material from these areas, instead sampling parts of the basaltic
293 boulder tops that showed fresh, unweathered surfaces. We recorded sample locations with a
294 handheld GPS unit or GAIA GPS (both with a vertical uncertainty of ± 5 m) and measured
295 topographic shielding in the field with a clinometer and compass.

6

Formatted: Default Paragraph Font, Font: +Body (Calibri), Font color: Black

Formatted: Default Paragraph Font, Font: +Body (Calibri), Font color: Black

Formatted: Normal, Right, Border: Top: (No border), Bottom: (No border), Left: (No border), Right: (No border), Between : (No border), Tab stops: 3.25", Centered + 6.5"; Right, Position: Horizontal: Left, Relative to: Column, Vertical: In line, Relative to: Margin, Wrap Around

Formatted: Font: Calibri, Font color: Black

Deleted:). These included 11 bedrock and 18 boulder samples...

Deleted: ranged

Deleted: in press

Deleted: allows

Deleted: , which helps interpret our suite of ¹⁰Be ages

Deleted: Island

Deleted: a similar composition

Deleted: a Pleistocene-aged basalt flow mapped on southwestern Suemez Island by

Deleted: . (

Deleted: However, we

Deleted: these

Deleted: elsewhere

311

3.2 ¹⁰Be dating

313

314

315

316

317

318

319

320

321

322

323

324

325

326

327

3.3 ³⁶Cl dating

329

330

331

332

333

334

335

We processed samples at the University at Buffalo Cosmogenic Isotope Laboratory

following established quartz purification and beryllium extraction procedures (e.g., Corbett et al.,

2016). After quartz purification, we dissolved samples in hydrofluoric acid with precisely

weighed ⁹Be carrier (PRIME Lab 2017.11.17-Be #3/#4; ⁹Be concentration of 1074 ± 8 ppm). We

isolated, oxidized, and packed beryllium into target cathodes in five different batches for

accelerator mass spectrometer (AMS) analysis at PRIME lab at Purdue University. The samples

were measured with respect to the 07KNSTD standard (¹⁰Be/⁹Be ratio of 2.85 x 10⁻¹²; Nishiizumi

et al., 2007). We corrected sample ratios using batch-specific blank values between 7.50 x 10⁻¹⁶

and 3.14 x 10⁻¹⁵. AMS analytical uncertainty ranged from 3.2 to 7.3% with an average value of

4.7%.

We calculated all ¹⁰Be ages using version 3 of the CRONUS-Earth exposure age

calculator (hess.ess.washington.edu; Balco et al., 2008; Balco, 2017), using the Arctic production

rate (Young et al., 2013) and a time-dependent (Lm) scaling scheme (Lal, 1991).

All whole rock samples were prepared at the University of New Hampshire Cosmogenic

Isotope Laboratory using a modified version of the protocols in Stone et al. (2000) and Licciardi

et al. (2008). After samples were crushed, etched in nitric acid, and homogenized, total sample

chloride was measured on a ~1 g aliquot of rock that was spiked with a small amount of ³⁷Cl-

enriched solution (LLNL Spike A; ³⁵Cl/³⁷Cl = 0.93; 1285 ± 3 ppm Cl) and a carrier containing

~4000 µg of Br. Cl was extracted as Ag(Cl,Br) following standard procedures and chlorine

7

Formatted: Default Paragraph Font, Font: +Body (Calibri), Font color: Black

Formatted: Default Paragraph Font, Font: +Body (Calibri), Font color: Black

Formatted: Normal, Right, Border: Top: (No border), Bottom: (No border), Left: (No border), Right: (No border), Between : (No border), Tab stops: 3.25", Centered + 6.5"; Right, Position: Horizontal: Left, Relative to: Column, Vertical: In line, Relative to: Margin, Wrap Around

Formatted: Font: Calibri, Font color: Black

Deleted: Samples

Deleted: to a 125-250 µm grain size, then rinsed

Deleted: deionized water

Deleted: leached in a weak HNO₃ solution to remove organic material. Each leached sample was

Deleted: using a riffle splitter and a ~1.2 g aliquot was removed to determine

Deleted: . The aliquots were

Formatted: Not Superscript/ Subscript

Formatted: Not Superscript/ Subscript

Formatted: Not Superscript/ Subscript

Deleted:). Aliquots also received

Deleted: (in the form of NH₄Br), which served to increase the size of the final precipitate. The aliquots were then dissolved in a solution of HF

Deleted: HNO₃. After dissolution, fluoride compounds were removed by centrifuging. Ag(Cl+Br) was precipitated

350 concentrations were determined through isotope dilution of $^{35}\text{Cl}/^{37}\text{Cl}$ ratios (Faure, 1986). ^{36}Cl
351 was extracted from full rock samples as Ag(Cl,Br) after adding a carrier containing ~4800 μg of
352 Br and a natural ratio Cl carrier ($^{35}\text{Cl}/^{37}\text{Cl} = 3.127$; 1436 ± 9 ppm Cl) to increase the size of the
353 final precipitate.
354 $^{35}\text{Cl}/^{37}\text{Cl}$ and $^{36}\text{Cl}/\text{Cl}$ ratios were measured at the Center for Accelerator Mass
355 Spectrometry at Lawrence Livermore National Laboratory. Analytical uncertainty on $^{35}\text{Cl}/^{37}\text{Cl}$
356 measurements ranged from 0.04% to 0.43%; analytical uncertainty on $^{36}\text{Cl}/\text{Cl}$ measurements
357 ranged from 2.12% to 2.87%. Major and trace element analyses were conducted by SGS
358 Minerals Services in Burnaby, British Columbia, Canada. Reported total Cl and ^{36}Cl
359 concentrations are corrected for batch-specific process blanks (Table 2). Analytical data used to
360 determine surface exposure ages are provided in supplementary tables S1 and S2. ^{36}Cl exposure
361 ages were calculated using an in-development version of the CRONUS-Earth ^{36}Cl calculator
362 (http://stoneage.ice-d.org/math/Cl36/v3/v3_Cl36_age_in.html) and Lm scaling (Lal, 1991).
363

364 3.4 Exposure age calculation considerations 365

366 We made no corrections for post-glacial elevation changes or snow cover when
367 calculating our ^{10}Be and ^{36}Cl ages. Post-glacial isostatic adjustment results in a time-varying rate
368 of cosmogenic nuclide production (Jones et al., 2019). This effect can be corrected for using
369 comprehensive records of regional emergence constrained by glacial isostatic adjustment models
370 or relative sea-level histories. Hundreds of radiocarbon ages constrain the relative sea level
371 chronology in the Alexander Archipelago; the sites in our study experienced ~50 m of relative
372 sea level lowering due to forebulge collapse between ~15 and 10 ka (Baichtal et al., 2021).
373 Corrections for glacial isostatic adjustment history, albeit slightly uncertain given site-to-site

8

Formatted: Default Paragraph Font, Font: +Body (Calibri), Font color: Black

Formatted: Normal, Right, Border: Top: (No border), Bottom: (No border), Left: (No border), Right: (No border), Between: (No border), Tab stops: 3.25", Centered + 6.5", Right, Position: Horizontal: Left, Relative to: Column, Vertical: In line, Relative to: Margin, Wrap Around

Formatted: Default Paragraph Font, Font: +Body (Calibri), Font color: Black

Formatted: Font: Calibri, Font color: Black

Deleted: the addition of AgNO₃. The Ag(Cl+Br) precipitates were recovered, rinsed, and packed into stainless steel cathodes for measurement

Deleted: , which were used to calculate total sample chloride by isotope dilution methods

Deleted: For the

Formatted: Not Superscript/ Subscript

Formatted: Not Superscript/ Subscript

Formatted: Not Superscript/ Subscript

Deleted: extraction,

Deleted: received

Deleted: small amount

Deleted: -

Formatted: Not Superscript/ Subscript

Deleted: ensure consistent Cl loads within the analytical batch. All samples received ~4800 μg of Br. The samples were dissolved in an HF-HNO₃ solution and insoluble fluorides were removed through centrifuging. Ag(Cl+Br) was precipitated by adding AgNO₃. The Ag(Cl+Br) precipitates were recovered and dissolved in a solution of NH₄OH. To remove ^{36}S , an isobar of ^{36}Cl , BaNO₃ was added to the solutions to precipitate BaSO₄. The purified Ag(Cl+Br) was precipitated by acidifying the solutions with HNO₃ and adding AgNO₃. The Ag(Cl+Br) precipitates were then recovered, rinsed, and dried.

Formatted: Not Superscript/ Subscript

Deleted: For comparison, ^{36}Cl ages calculated using version 2.1 of CRONUScalc (Marrero et al., 2016a) are included in supplementary table S3.

Deleted: , post-depositional erosion,

Deleted: glacier

Deleted:

Deleted: in press

Deleted: this

403 differences in elevation history, result in small changes (~1% age decrease), and thus we report
404 our ages without any correction for isostatic adjustment (Tables 1 and 2). Furthermore, changes
405 in air pressure near a retreating ice margin and shifts in air compression above a sample site that
406 experienced elevation change may mitigate any effects of isostatic adjustment on cosmogenic
407 nuclide production, potentially rendering any elevation correction unnecessary (Staiger et al.,
408 2007).

409 Extended periods of thick and dense snow cover can also inhibit ^{10}Be and ^{36}Cl production
410 in a rock surface and lead to erroneously young apparent exposure ages. While modern snowfall
411 reports for lower-elevation areas of the Alexander Archipelago indicate minimal average
412 wintertime snow cover (10 – 20 cm; [https://wrcc.dri.edu/summary/](https://wrcc.dri.edu/summary/Climsmak.html) Climsmak.html), there are no
413 data for higher-elevation areas. Consequently, we cannot report our ages with reliable snow
414 shielding corrections and these exposure dates should be considered minimum ages. However,
415 most of our sites are from low to moderate elevations (<500 m asl; Table 1).

416 Post-depositional weathering and erosion can also affect exposure ages. We observed
417 fresh, unweathered glacially scoured bedrock across all our field sites, indicating minimal post-
418 glacial erosion. We made no corrections for erosion in our age calculations presented within the
419 manuscript text and thus these should be considered minimum ages. For sensitivity purposes, we
420 calculated ages using an erosion rate of 0.3 cm/kyr, similar to erosion rates applied nearby in
421 British Columbia (Menounos et al., 2017). These erosion-corrected ages are between 2% and 7%
422 older and are found in Tables S3 and S4.

423 Both cosmogenic and nucleogenic ^{36}Cl can be present in rock surfaces, and for our
424 surface exposure age calculations we assumed steady state production/decay of nucleogenic ^{36}Cl .
425 Moderate amounts of nucleogenic ^{36}Cl are produced when ^{35}Cl absorbs neutrons released by the

9

Formatted: Normal, Right, Border: Top: (No border), Bottom: (No border), Left: (No border), Right: (No border), Between : (No border), Tab stops: 3.25", Centered + 6.5", Right, Position: Horizontal: Left, Relative to: Column, Vertical: In line, Relative to: Margin, Wrap Around

Formatted: Default Paragraph Font, Font: +Body (Calibri), Font color: Black

Formatted: Default Paragraph Font, Font: +Body (Calibri), Font color: Black

Formatted: Font: Calibri, Font color: Black

Moved down [1]: Post-depositional weathering and erosion can also affect exposure ages. We observed fresh, unweathered glacially scoured bedrock across all our field sites, indicating minimal post-glacial erosion.

Deleted: Therefore, we made no corrections for erosion in our age calculations.

Deleted:

Formatted: Font: Times New Roman, 12 pt

Moved (insertion) [1]

Formatted: Default Paragraph Font, Font: +Body (Calibri), Font color: Black

Formatted: Normal, Right, Border: Top: (No border), Bottom: (No border), Left: (No border), Right: (No border), Between : (No border), Tab stops: 3.25", Centered + 6.5", Right, Position: Horizontal: Left, Relative to: Column, Vertical: In line, Relative to: Margin, Wrap Around

Formatted: Default Paragraph Font, Font: +Body (Calibri), Font color: Black

Formatted: Font: Calibri, Font color: Black

433 [decay of U and Th isotopes \(Gosse and Phillips, 2001\). However, because the formation age of](#)
 434 [the sampled basalt flow on Suemez Island is loosely constrained to the “Tertiary to Quaternary”](#)
 435 [\(Eberlein et al., 1983\), nucleogenic ³⁶Cl production/decay may or may not be in steady state. To](#)
 436 [assess the sensitivity of our exposure ages to the assumption of steady state nucleogenic ³⁶Cl](#)
 437 [production, we also calculated exposure ages using a rock formation age of 20 ka, which, given](#)
 438 [the timing of the LLGM ice advance in Southeast Alaska \(Lesnek et al., 2018\), is the youngest](#)
 439 [formation age we might expect for these rocks. Results of this test \(Table S3\) show that](#)
 440 [calculated ³⁶Cl ages are relatively insensitive to rock formation age \(<1% surface exposure age](#)
 441 [increase in all cases\), which is well within total uncertainty.](#)

442

443 **4 Results**

444

445 We sampled from the summit of a massif at ~410 m asl on south-central Suemez Island
 446 (southern Alexander Archipelago) and from a flat bench scattered with boulders on the summit’s
 447 flank for ¹⁰Be dating (Fig. 6). The two boulders sampled on the bench date to 15.6 ± 0.7
 448 (19SEAK-07; Fig. 3) and 15.0 ± 1.1 ka (19SEAK-08; we report all surface exposure ages with 1
 449 σ internal uncertainty; Table 1). The summit site featured fresh glacially sculpted bedrock
 450 surfaces with a couple boulders resting on the bedrock. A boulder and its adjacent bedrock
 451 surface, as a pair, date to 17.4 ± 1.2 (19SEAK-09) and 19.7 ± 1.2 ka (19SEAK-10), respectively
 452 (Fig. 3). The three boulders yield a mean age of 16.0 ± 1.2 ka (n = 3; 1 SD).

Deleted: .).

453 On southwestern Suemez Island, we sampled four large boulders for ³⁶Cl dating. The
 454 boulders were distributed across a terrain of patchy muskeg with locally outcropping bedrock.
 455 Based on reconstructed [Cordilleran Ice Sheet](#) flow directions (Lesnek et al., 2020) and boulder
 456 composition (supplementary table S2; Eberlein et al., 1983), the boulders were likely plucked

Deleted: CIS

459 from basalt flows present on the southwestern portion of Suemez Island (Brew, 1996). The four
 460 basalt boulders from southwestern Suemez Island have ^{36}Cl exposure ages ranging from $12.4 \pm$
 461 0.3 to 16.4 ± 0.5 ka (ages are reported at 1σ internal uncertainty; Fig. 5; Table 2). ^{36}Cl surface
 462 exposure ages assuming 3 mm/ka of surface erosion and non-steady state nucleogenic ^{36}Cl
 463 production are presented in Table S3; for all four samples, changing these parameters results in
 464 calculated surface exposure ages <2% higher than those presented in the main text.

465 We collected samples from four sites (Baranof Sites A – D; Fig. 7) on the ocean-facing
 466 side of Baranof Island, northern Alexander Archipelago. Here, we chose our helicopter ground
 467 stops in an area previously mapped as ice-free throughout the [LLGM](#) (Carrara et al., 2007; Fig.
 468 7). Evidence for glacial sculpting of bedrock surfaces is clear; glacial grooves, striations and
 469 chatter marks are present at all sites, and the bedrock surfaces, in places, are topped by perched
 470 boulders (Fig. 3). Field evidence of recent glaciation, including relatively unweathered chatter
 471 marks, grooves, and striations, contradicts prior mapping of these areas being ice-free during the
 472 [LLGM](#).

473 Baranof Site A is a large, unforested area of bedrock outcrops composed of several
 474 smaller ridges. Here, we sampled two bedrock surfaces – one from the stoss side of a bedrock
 475 outcrop (19SEAK-18; Fig. 3) and one from the top surface of a nearby bedrock patch (19SEAK-
 476 19) – which date to 21.7 ± 0.9 and 28.0 ± 1.1 ka, respectively. A boulder sampled adjacent to
 477 bedrock (sample 19SEAK-18) yielded an exposure age of 16.9 ± 0.8 ka (19SEAK-17). A second
 478 boulder sample from this [site](#) dates to 14.4 ± 0.7 ka (19SEAK-20; Fig. 3). At Baranof Site B – a
 479 raised bedrock knob – we sampled two boulders and one bedrock surface. The two boulders have
 480 ^{10}Be ages of 15.1 ± 0.6 ka (19SEAK-23; Fig. 3), 14.4 ± 0.7 ka (19SEAK-21); the bedrock [sample](#)
 481 has a ^{10}Be age of 14.4 ± 0.6 ka (19SEAK-22). Baranof Site C is a high ridge between the ocean

Formatted: Default Paragraph Font, Font: +Body (Calibri), Font color: Black

Formatted: Default Paragraph Font, Font: +Body (Calibri), Font color: Black

Formatted: Normal, Right, Border: Top: (No border), Bottom: (No border), Left: (No border), Right: (No border), Between: (No border), Tab stops: 3.25", Centered + 6.5"; Right, Position: Horizontal: Left, Relative to: Column, Vertical: In line, Relative to: Margin, Wrap Around

Formatted: Font: Calibri, Font color: Black

Deleted:

Deleted: 5 ± 1.1

Deleted: 6 ± 1.6

Deleted: ILGM

Deleted: ILGM

Deleted: stop

Deleted: samples

489 and a U-shaped valley with abundant bedrock outcrops and few boulders. Here, a boulder yielded
490 an exposure age of 16.3 ± 0.6 ka (19SEAK-24; Fig. 3) whereas a bedrock surface dates to $15.7 \pm$
491 0.6 ka (19SEAK-25). Finally, Baranof Site D is a small bedrock ridge between two peaks with
492 massive stoss and lee features. At this site, we collected samples from two quartz veins in the
493 bedrock, which have exposure ages of 18.2 ± 0.7 (19SEAK-26; Fig. 3) and 20.2 ± 0.8 ka
494 (19SEAK-27). Because the sites are all in relatively close proximity and from similar elevations
495 (50 – 160 m asl), we treat the samples as having experienced the same glacial history, and thus
496 should belong to a single age population. Collectively, boulder samples yield a mean age of 15.4
497 ± 1.1 ka ($n = 5$; 1 SD) with no obvious outliers, whereas the bedrock samples exhibit more scatter
498 and are mostly older than the mean boulder age (Fig. 9).

499 Biorka Island, a small island off the western coast of central Baranof Island, was initially
500 mapped as ice-covered throughout the LLGM (Dyke, 2004). Here, there are numerous ~1 m tall
501 boulders that rise above the surrounding vegetation and rest on ice-sculpted bedrock. Vegetation
502 and sediments mostly obscure underlying bedrock surfaces, and thus we only collected samples
503 from boulders at this sampling site. Our four boulder samples yielded exposure ages of $15.3 \pm$
504 0.5 (18JB005; Fig. 4), 14.9 ± 0.6 (18JB006), 15.4 ± 0.5 (18JB007; Fig. 4), and 13.7 ± 0.5 ka
505 (18JB008), with a mean of 14.8 ± 0.8 ka ($n = 4$; 1 SD; Fig. 8).

506 We visited a summit ridge at 545 – 560 m asl on the western, ocean-facing side of
507 northwestern Kruzof Island, previously mapped as ice-free throughout the LGM (Dalton et al.,
508 2020). There, we found many large stable boulders and exposed patches of glacially sculpted
509 bedrock between vegetation exhibiting glacial grooves and chatter marks. Here, we sampled
510 three large boulders ($> 2 \times 2 \times 1$ m), which date to 14.9 ± 0.8 (20SEAK-07; Fig. 4), 14.9 ± 0.9
511 (20SEAK-12) and 14.6 ± 0.8 ka (20SEAK-13; Fig. 4), yielding a mean age of 14.8 ± 0.2 ka ($n =$

12

Formatted: Default Paragraph Font, Font: +Body (Calibri), Font color: Black

Formatted: Normal, Right, Border: Top: (No border), Bottom: (No border), Left: (No border), Right: (No border), Between : (No border), Tab stops: 3.25", Centered + 6.5", Right, Position: Horizontal: Left, Relative to: Column, Vertical: In line, Relative to: Margin, Wrap Around

Formatted: Default Paragraph Font, Font: +Body (Calibri), Font color: Black

Formatted: Font: Calibri, Font color: Black

Deleted: ILGM

513 3; 1 SD; Fig. 8). A bedrock surface at this site dates to 13.4 ± 1.0 ka (20SEAK-10; Fig. 4) and
514 sits ~10 m below and ~10 m away from the boulder that dated to 14.6 ± 0.8 ka (20SEAK-13).

515 We collected samples from three sites on Chichagof Island (Chichagof Sites A – C; Fig.
516 8). Unlike our other sampling locations which are on the ocean-facing, western sides of the
517 archipelago, the Chichagof Island sites are all located inland. We visited these sites to determine
518 the timing of ice retreat inland and to complement the findings of a previous study that
519 documented ice withdrawal in the central and eastern Alexander Archipelago (Lesnek et al.,
520 2020). Chichagof Island is notable for its relative lack of boulders – consequently, the boulders
521 sampled here are smaller than those at other sites. While many bedrock outcrops featured smooth
522 surfaces indicative of glacial erosion, we did not observe clear striations or chatter marks. At site
523 A, a bedrock bench, ^{10}Be ages from two small, perched boulders are 12.7 ± 0.7 (20SEAK-15; 0.5
524 x 0.3 x 0.3 m; 476 m asl; Fig. 4) and 9.0 ± 0.6 ka (20SEAK-16; 0.5 x 0.4 x 0.3 m; 473 m asl). A
525 quartz vein sampled from bedrock outcrop at this site has an exposure age of 15.3 ± 0.7 ka
526 (20SEAK-14). Site B is a series of bedrock ridges, and a single boulder yields an exposure age of
527 12.4 ± 0.9 ka (20SEAK-18; 817 m asl; Fig. 4), while an adjacent bedrock surface dates to $14.1 \pm$
528 0.7 ka (20SEAK-19; 816 m asl). Finally, site C is at the summit of a massif and one bedrock
529 knob sampled here has an exposure age of 17.7 ± 0.8 ka (20SEAK-22; 779 m asl; Fig. 4).

530

531 **5 Discussion**

532

533 **5.1 Bedrock ^{10}Be ages**

534

535 We sampled large and stable boulders in addition to bedrock surfaces with clear evidence of

536 glacial erosion (e.g., striations, chatter marks) with the goal of providing optimal constraints on

537 deglaciation. Sampling bedrock surfaces also allows us to better understand the subglacial

13

Formatted: Default Paragraph Font, Font: +Body (Calibri), Font color: Black

Formatted: Normal, Right, Border: Top: (No border), Bottom: (No border), Left: (No border), Right: (No border), Between: (No border), Tab stops: 3.25", Centered + 6.5", Right, Position: Horizontal: Left, Relative to: Column, Vertical: In line, Relative to: Margin, Wrap Around

Formatted: Default Paragraph Font, Font: +Body (Calibri), Font color: Black

Formatted: Font: Calibri, Font color: Black

Deleted:

539 erosion regime across the Alexander Archipelago, potentially yielding information about the
540 duration of ice cover, the amount of subglacial erosion, and the likelihood of boulders containing
541 inheritance.

542 Bedrock exposure ages are older than the mean boulder exposure ages by two SD or
543 greater on Suemez Island (19SEAK-10) and Baranof sites A (19SEAK-18, 19SEAK-19) and D
544 (19SEAK26, 19SEAK-27). At Chichagof site A the bedrock exposure age (20SEAK-14) is ~4.5
545 kyr older than the mean boulder age, but still within two standard deviations, perhaps due to the
546 large spread in boulder ages resulting in larger standard deviations. At Chichagof site B, the
547 single boulder ¹⁰Be age (20SEAK-18) post-dates the single bedrock age by ~1.7 kyr. In general,
548 bedrock data reported here are consistent with bedrock ¹⁰Be ages from Warren and Baker islands
549 that are older (by more than 2 SD) than mean boulder ages (Lesnek et al., 2018). Bedrock ages
550 may be erroneously older due to ¹⁰Be inheritance if ice sheet erosion was insufficient to remove
551 the ~2 m of rock required to remove most of the previous ¹⁰Be inventory. Studies from British
552 Columbia (Darvill et al., 2018) and Washington (Briner and Swanson, 1998) also report
553 cosmogenic nuclide inheritance in bedrock from other areas covered by the [Cordilleran Ice](#)
554 [Sheet](#). In our field area, the short-lived nature of the overriding event (~3 kyr; Lesnek et al.,
555 2018) may also contribute to the lack of significant glacial erosion. Finally, traces of inheritance
556 may be present in bedrock, perhaps even boulders, in ice-sheet-distal sites like these that are
557 overrun by ice during extremely brief portions of the Quaternary (Briner et al., 2016).

558 In some cases, boulder-bedrock pairs have similar exposure ages (on southern Baranof
559 and Suemez islands), suggesting our bedrock ages are unaffected by ¹⁰Be inheritance at these
560 sites. On Kruzof Island, a bedrock patch yields an exposure age that is younger (by more than 2
561 σ) than the mean age of the surrounding boulders. Potential cover by snow, sediment, or

14

Formatted: Default Paragraph Font, Font: +Body (Calibri), Font color: Black

Formatted: Normal, Right, Border: Top: (No border), Bottom: (No border), Left: (No border), Right: (No border), Between : (No border), Tab stops: 3.25", Centered + 6.5", Right, Position: Horizontal: Left, Relative to: Column, Vertical: In line, Relative to: Margin, Wrap Around

Formatted: Default Paragraph Font, Font: +Body (Calibri), Font color: Black

Formatted: Font: Calibri, Font color: Black

Deleted: CIS.

565 vegetation is thought to have caused anomalously young ages elsewhere in the Alexander
566 Archipelago (Lesnek et al., 2020) and may also explain this ^{10}Be age from our bedrock site on
567 Kruzof Island.

568 Bedrock exposure ages vary greatly (by as much as ~14 kyr) between the various
569 sampling locations on Baranof Island and up to 6 kyr on Suemez Island (Lesnek et al., 2018).
570 The Alexander Archipelago is characterized by impressive relief (deep fjords, high peaks), and
571 thus, sub-glacial erosion rates clearly varied greatly across Suemez and Baranof islands where
572 sampling locations are ~2 – 6 km apart. Differing bedrock ^{10}Be ages from the same sampling
573 locales confirm this [inference](#), reflecting variable sub-glacial erosion rates even within ~100 m of
574 each other. Some samples may have been collected in areas dominated by glacial abrasion,
575 whereas other samples might be from surfaces dominated by quarrying, and thus, this variability
576 could reflect varying subglacial processes on a local scale.

577 Because bedrock exposure ages from the coastal Alexander Archipelago (this study;
578 Lesnek et al., 2018) do not consistently pre-date, match, or post-date exposure ages from
579 adjacent boulders, we refrain from including bedrock-based ^{10}Be ages in our mean [deglaciation](#)
580 age calculations (Figs. 9; 10). This negates biases when choosing which bedrock ages “match”
581 nearby erratic ages and allows us to eliminate any concern over inheritance or post-ice retreat
582 cover of these bedrock surfaces. While bedrock ages, especially when paired with boulder ages,
583 are useful for identifying spatially variable subglacial erosion processes and issues with past
584 cover and inheritance, they do not [appear to](#) provide reliable age constraints on the timing of
585 deglaciation [in the Alexander Archipelago due to the inconsistencies between bedrock and](#)
586 [boulder ages](#). In light of this, we also recalculate relevant mean ages from Lesnek et al. (2018;
587 2020) using solely boulder ^{10}Be ages to update these other regional chronologies.

15

Formatted: Normal, Right, Border: Top: (No border), Bottom: (No border), Left: (No border), Right: (No border), Between: (No border), Tab stops: 3.25", Centered + 6.5", Right, Position: Horizontal: Left, Relative to: Column, Vertical: In line, Relative to: Margin, Wrap Around

Formatted: Default Paragraph Font, Font: +Body (Calibri), Font color: Black

Formatted: Default Paragraph Font, Font: +Body (Calibri), Font color: Black

Formatted: Font: Calibri, Font color: Black

588 **5.2 ¹⁰Be chronology incompatible with mapped Cordilleran Ice Sheet extent**

589

590 We targeted areas of the northern Alexander Archipelago mapped as ice-free by previous
591 studies to determine whether these areas were [LLGM](#) refugia. The most recent coastal
592 [Cordilleran Ice Sheet](#) reconstructions show significant portions of the northern Alexander
593 Archipelago as remaining ice-free throughout the [LLGM](#) (Fig. 2), with ice terminating close to
594 the present shoreline – not on the continental shelf (Dalton et al., 2020; Lesnek et al., 2020). Our
595 data, however, indicate that at least some of these areas [previously](#) mapped as refugia
596 (southwestern Baranof and Kruzof islands) were covered by ice, and deglaciated around 15.4 –
597 14.8 ka. Our new evidence thus suggests that ice extended onto the continental shelf during the
598 [LLGM](#), as in the southern Alexander Archipelago (Lesnek et al., 2018). These discrepancies
599 between previously mapped ice extents and those implied by our new exposure ages highlight
600 the need to develop deglaciation chronologies elsewhere along the [Cordilleran Ice Sheet](#) coastal
601 margin to provide updated mapping around the north Pacific.

602

603 **5.3 Cordilleran Ice Sheet retreat across the Alexander Archipelago**

604

605 Mean boulder ¹⁰Be exposure ages from Suemez Island in this study and Lesnek et al.
606 (2018), 16.4 ± 1.2 ka (n = 3 boulders; 1 SD) and 16.6 ± 0.8 ka (n = 3 boulders; 1 SD),
607 [respectively](#), overlap within 1 standard deviation (Figs. 6; 9). However, three of the boulder ³⁶Cl
608 ages from southwestern Suemez Island do not overlap with the ¹⁰Be ages at 1 standard deviation
609 (Figs. 6; 9). [We attribute this scatter to post-depositional surface erosion of the basaltic boulders](#)
610 [\(i.e., those dated with ³⁶Cl\) in excess of 3 mm/ka. Although we targeted areas of the boulder](#)
611 [tops with no obvious signs of erosion, given the maritime climate of Southeast Alaska it is](#)

16

Formatted: Default Paragraph Font, Font: +Body (Calibri), Font color: Black

Formatted: Default Paragraph Font, Font: +Body (Calibri), Font color: Black

Formatted: Normal, Right, Border: Top: (No border), Bottom: (No border), Left: (No border), Right: (No border), Between : (No border), Tab stops: 3.25", Centered + 6.5"; Right, Position: Horizontal: Left, Relative to: Column, Vertical: In line, Relative to: Margin, Wrap Around

Formatted: Font: Calibri, Font color: Black

Formatted: Indent: First line: 0.5"

Deleted: ILGM

Deleted: CIS

Deleted: ILGM

Deleted: that were

Deleted: ILGM

Deleted: CIS

Deleted: 0

Deleted: ,

Deleted:

621 [possible that the original, glacially eroded boulder surfaces have been weathered](#). Surface erosion
 622 of rocks with low concentrations of native Cl (supplementary table S2), where the primary ^{36}Cl
 623 production pathway is Ca-spallation (Marrero et al., [2016](#)), results in exposure ages that are
 624 erroneously young. Thus, we interpret the oldest ^{36}Cl exposure age (16.4 ± 0.5 ka; 19SEAK-02)
 625 as the closest constraint on deglaciation at that site. This ^{36}Cl age overlaps with the ^{10}Be ages
 626 from elsewhere on Suemez Island; we combine them and calculate a new, boulder-based mean
 627 deglaciation age of 16.3 ± 0.8 ka ($n = 10$ boulders; 1 SD) for Suemez Island.

628 We group together three of our sampling locations in the northern Alexander Archipelago
 629 that are ocean-facing: Kruzof, Biorka, and southern Baranof islands. As the [Cordilleran Ice Sheet](#)
 630 retreated from the continental shelf inland, these were the first areas presently above sea level to
 631 become ice-free. We calculate a mean ^{10}Be boulder age of 15.1 ± 0.9 ka ($n = 12$ boulders; 1 SD)
 632 for the coastal northern Alexander Archipelago.

633 There are limited data from elsewhere in the northern Alexander Archipelago that
 634 constrain the timing of deglaciation. A basal pollen concentrate-based radiocarbon age from
 635 Hummingbird Lake (Fig. 7), southwestern Baranof Island dates to 15.0 ± 0.2 [cal](#) ka, in
 636 agreement with the ^{10}Be ages presented here and that collectively indicate coastal Baranof Island
 637 was deglaciated prior to [~15 ka](#) (Ager, 2019). Additionally, tephra layers from Mt. Edgecumbe
 638 on Kruzof Island are dated to 13.1 ka (Riehle et al., 1992; Beget et al., 1998), and blanket many
 639 of the surrounding islands, suggesting that these areas were ice-free by then.

640 All three sample sites on Chichagof Island (Sites A – C) are not ocean-adjacent and
 641 characterized by a general lack of boulders. The boulders present were much smaller, and shorter
 642 (< 0.5 m high) than boulders sampled elsewhere across the Alexander Archipelago – we chose to
 643 sample these despite their size to provide minimum ages for deglaciation and to compare with

Formatted: Default Paragraph Font, Font: +Body (Calibri), Font color: Black

Formatted: Normal, Right, Border: Top: (No border), Bottom: (No border), Left: (No border), Right: (No border), Between : (No border), Tab stops: 3.25", Centered + 6.5", Right, Position: Horizontal: Left, Relative to: Column, Vertical: In line, Relative to: Margin, Wrap Around

Formatted: Default Paragraph Font, Font: +Body (Calibri), Font color: Black

Formatted: Font: Calibri, Font color: Black

Deleted: 2016b

Deleted:

Deleted: 6

Deleted:

Deleted: CIS

Deleted: this

Deleted: ,

Deleted: notably,

652 available radiocarbon constraints. The ages of these boulders fall between 9.0 ± 0.6 and $12.7 \pm$
 653 0.7 ka, and are thus younger than other age constraints for deglaciation on Chichagof Island;
 654 radiocarbon ages on shells from raised marine terraces on Chichagof Island date back to $14.2 \pm$
 655 0.6 cal ka suggesting that the island was ice-free by this time (Baichtal et al., 2021). Smaller
 656 boulders are more susceptible to cover (whether snow, vegetation, or sediment), and may thus
 657 yield anomalously young ^{10}Be ages. While a lack of large boulders found on Chichagof Island
 658 makes it difficult to ascertain the timing of deglaciation, regional glacial and sea-level history
 659 suggests Chichagof Island was deglaciated between 15.1 (when the coastal area deglaciated) and
 660 14.2 cal ka (the age of shells in raised marine deposits). Therefore, the boulders dated here likely
 661 have anomalously young exposure ages.

662 Our mean ^{10}Be age of 15.1 ± 0.9 ka ($n = 12$ boulders; 1 SD) from all sites along the
 663 coastal portion of the northern Alexander Archipelago, fits with the few other regional
 664 deglaciation constraints (Fig. 2) and overlaps within one standard deviation with the mean
 665 boulder exposure age from the southern Alexander Archipelago of 16.3 ± 0.8 ka ($n = 13$
 666 boulders; 1σ ; this study; Lesnek et al., 2018; Lesnek et al., 2020). While mean ages from the
 667 northern and southern Alexander Archipelago overlap within one standard deviation, it is
 668 possible that these areas deglaciated at slightly different times as these various sampling sites
 669 happened to become ice-free. Furthermore, local ice caps formed and radiated from massifs on
 670 Chichagof, Baranof, and Prince of Wales islands during the LIGM (Capps, 1932; Mann and
 671 Hamilton, 1995; Lesnek et al., 2020). These local ice caps served as a local ice source for the
 672 Alexander Archipelago and their locations and flow patterns may have led to some parts of the
 673 archipelago becoming ice-free before others. Thus, we present a range of deglaciation across the
 674 coastal Alexander Archipelago from between 16.3 ± 0.8 ka and 15.1 ± 0.9 ka

Formatted: Default Paragraph Font, Font: +Body (Calibri), Font color: Black

Formatted: Default Paragraph Font, Font: +Body (Calibri), Font color: Black

Formatted: Normal, Right, Border: Top: (No border), Bottom: (No border), Left: (No border), Right: (No border), Between : (No border), Tab stops: 3.25", Centered + 6.5"; Right, Position: Horizontal: Left, Relative to: Column, Vertical: In line, Relative to: Margin, Wrap Around

Formatted: Font: Calibri, Font color: Black

Deleted: radio carbon

Deleted: They date

Deleted: . Their ages

Deleted: in press

Deleted: make

Deleted:

Deleted: our

Deleted: of 15.1 ± 0.9 ka ($n = 12$ boulders; 1 SD)

Deleted: ¶

Deleted: ILGM

685 Ice retreat across the Alexander Archipelago is also registered in marine sediments off
686 the former coastal [Cordilleran Ice Sheet](#) margin. Several marine sedimentary records (cores
687 EW0408-26JC, EW0408-66JC, EW0408-85JC) extending back to ~18.5 cal ka show the
688 presence of IRD beginning ~18.5 ka, peaking at 17.5 – 16.5 ka and ceasing at 14.8 ka, reflecting
689 a final retreat of marine-terminating ice (Praetorius and Mix, 2014). Furthermore, these IRD data
690 record fluctuating but relatively elevated calving spanning 18.5 to 14.8 ka, perhaps indicating
691 steady retreat punctuated by periods of accelerated melting.

692 Tephra from Mt. Edgumbe (Kruzof Island) found in core EW0408-26JC is interpreted
693 ~~to have been~~ deposited in a submarine environment, suggesting that this core site was ice-free by
694 14.6 ka (Praetorius et al., 2016). Records of a subsequent eruption dated to ~13.1 cal ka from
695 marine sediments in Sitka Sound (core EW0408-40JC) indicate that this area (between Baranof
696 and Kruzof islands) must have been ice-free by this time (Addison et al., 2010). Finally, ¹⁴C ages
697 from mollusks found in a diamicton layer along the Gastineau Channel date to ~13.8 cal ka,
698 reflecting the beginning of deglaciation near the mainland (Miller, 1973; we calibrate all
699 uncalibrated ¹⁴C ages with CALIB 8.2; Stuiver et al., 2021).

701 5.4 Chronologies of Cordilleran Ice Sheet deglaciation across the North Pacific

702
703 Radiocarbon ages from the [Cordilleran Ice Sheet](#) margin reflect ice advance from ~20 – 17 ka,
704 near the end of the [GLGM](#) at 19 ka. [Ages from](#) mammalian fossils in Shuká Káa on Prince of
705 Wales Island indicate [Cordilleran Ice Sheet](#) advance ~20 ka in the Alexander Archipelago
706 (Lesnek et al., 2018). Directly south of the Alexander Archipelago, on eastern Graham Island
707 (Haida Gwaii) initial ice advance is dated to 24.1 – 22.5 cal ka with a ¹⁴C date from a twig
708 underlying [till](#) (Blaise et al., 1990; Mathewes and Clague, 2017). Along the southwestern

19

Formatted: Default Paragraph Font, Font: +Body (Calibri), Font color: Black

Formatted: Default Paragraph Font, Font: +Body (Calibri), Font color: Black

Formatted: Normal, Right, Border: Top: (No border), Bottom: (No border), Left: (No border), Right: (No border), Between : (No border), Tab stops: 3.25", Centered + 6.5"; Right, Position: Horizontal: Left, Relative to: Column, Vertical: In line, Relative to: Margin, Wrap Around

Formatted: Font: Calibri, Font color: Black

Deleted: CIS

Deleted: as being

Deleted: CIS

Deleted: gLGM

Deleted: Dates from

Deleted: CIS

Deleted: glacial

716 [Cordilleran Ice Sheet](#) margin, ice reached its maximum extent until ~17.0 ka in the Puget Sound
 717 area (Porter and Swanson, 1998).

718 Glacier chronologies from the northeastern Pacific coastline also reflect post-[GLGM](#)
 719 retreat. On Sanak Island, tephra near the bottom of a lake sediment core dates deglaciation before
 720 ~15.9 ka, [broadly synchronous with Cordilleran Ice Sheet](#) withdrawal in the Alexander
 721 Archipelago (Misarti et al., 2012). On Kodiak Island, final [LLGM](#) retreat dates to ~15.7 cal ka,
 722 as marked by a ¹⁴C age above glacio-tectonically altered sediments (Mann and Peteet, 1994).
 723 Directly north of the Alexander Archipelago, a ¹⁴C age from a log found within the Finger
 724 Glacier lateral moraine provides a minimum [age of deglaciation](#) at ~14.6 cal ka (Mann, 1986).
 725 Radiocarbon ages from a marine sediment core in Dixon Entrance date maximum [Cordilleran Ice](#)
 726 [Sheet](#) extent to before ~16.1 cal ka and retreat beginning before ~15.3 cal ka (Barrie and
 727 Conway, 1999). A marine sediment record from Vancouver Sound similarly dates maximum ice
 728 extent to 18.5 ka and retreat of the [Cordilleran Ice Sheet](#) onto the mainland by 16.4 ka (Blaise et
 729 al., 1990). Quaternary sediments on eastern Graham Island indicate the [Cordilleran Ice Sheet](#) was
 730 retreating by 17.8 cal ka (Blaise et al., 1990). Notably, ¹⁰Be ages on Calvert Island suggest ice
 731 retreated off the continental shelf at ~18 ka, pre-dating ice withdrawal onto land in the Alexander
 732 Archipelago (Darvill et al., 2018).

733 Marine sediment cores are interpreted to show ice retreat across the coastal northeastern
 734 Pacific. A marine sediment core (SO202-27-6) from the Gulf of Alaska captures a decrease in
 735 sea surface salinity ~16 ka, interpreted to reflect increased meltwater from the [Cordilleran Ice](#)
 736 [Sheet](#) margin (Maier et al., 2018). Another marine sediment core (EW0408-85JC) [recovered](#) off
 737 the coast of southern Alaska records a decrease in glacial-margin sediment accumulation at 16.9
 738 ka as ice stagnated or began to retreat. (Davies et al., 2011). Reductions in salinity captured by

Formatted: Default Paragraph Font, Font: +Body (Calibri), Font color: Black

Formatted: Default Paragraph Font, Font: +Body (Calibri), Font color: Black

Formatted: Normal, Right, Border: Top: (No border), Bottom: (No border), Left: (No border), Right: (No border), Between : (No border), Tab stops: 3.25", Centered + 6.5"; Right, Position: Horizontal: Left, Relative to: Column, Vertical: In line, Relative to: Margin, Wrap Around

Formatted: Font: Calibri, Font color: Black

Deleted: CIS

Deleted: 18.3 ka in the Coquitlam Valley and ~

Deleted: Clague et al., 1980;

Deleted: gLGM

Deleted: prior to the onset of CIS

Deleted: ILGM

Deleted: constraint on

Deleted: CIS

Deleted: CIS

Deleted: CIS

Deleted: CIS

Deleted: from

751 planktonic $\delta^{18}\text{O}$ in this core at ~ 16.7 ka are interpreted as an increase in meltwater input from
 752 retreating glaciers. A transition from ice-proximal to laminated hemipelagic sediments at ~ 14.8
 753 ka marks glacier retreat off the continental shelf and onto land. [Off the coast of Alaska, a marine
 754 sediment core records a peak of IRD deposition peaking between 18 and 17 ka, interpreted as the
 755 retreat of marine-terminating margins of the Cordilleran Ice Sheet \(Walczak et al., 2020\).](#)
 756 [Additionally, another](#) core from off Vancouver Island (MD02-2496) captures IRD deposition
 757 between ~ 17.0 and ~ 16.2 cal ka – indicating rapid regional deglaciation – and a minor IRD event
 758 at ~ 14.7 cal ka (Cosma et al., 2008).

759 Our new data showing ice retreat at 15.1 ± 0.9 ka from the northern Alexander
 760 Archipelago, along with ages of deglaciation from the southern Alexander Archipelago ($16.3 \pm$
 761 0.8 ka; this study; Lesnek et al., 2018), are broadly synchronous with previously published ice
 762 retreat chronologies for the marine-terminating [Cordilleran Ice Sheet](#) margin elsewhere along the
 763 northeast Pacific Coast. However, while our chronology only documents deglaciation, it provides
 764 further evidence of a delayed [LLGM](#) across the coastal [Cordilleran Ice Sheet](#) compared to the
 765 [GLGM](#) maximum extents of alpine glaciers in mainland Alaska (Briner et al., 2017), parts of
 766 southern Alaska (Reger et al., 1996), and the [Laurentide Ice Sheet](#) (Dalton et al., 2020).

768 5.5 Paleoclimate Records from the North Pacific

769
 770 Several paleoclimate records from around the North Pacific span our interval of [Cordilleran Ice
 771 Sheet](#) deglaciation in the Alexander Archipelago. A combined diatom assemblage- and alkenone-
 772 derived record of sea surface temperatures (SSTs) from the Bering Sea (Core 51JPC), records
 773 perennial sea ice from ~ 22.5 ka (beginning of record) to 17 ka, and increased SSTs beginning
 774 ~ 16.9 ka before a notable shift back to annual sea ice ~ 16.7 ka (Caissie et al., 2010). In the

Formatted: Default Paragraph Font, Font: +Body (Calibri), Font color: Black

Formatted: Default Paragraph Font, Font: +Body (Calibri), Font color: Black

Formatted: Normal, Right, Border: Top: (No border), Bottom: (No border), Left: (No border), Right: (No border), Between: (No border), Tab stops: 3.25", Centered + 6.5", Right, Position: Horizontal: Left, Relative to: Column, Vertical: In line, Relative to: Margin, Wrap Around

Formatted: Font: Calibri, Font color: Black

Deleted: Additionally, a marine sediment

Deleted: CIS

Deleted: ILGM

Deleted: CIS

Deleted: gLGM

Deleted: LIS

Deleted: CIS

782 northern Gulf of Alaska (Core EW0408-85JC), $\delta^{18}\text{O}$ data document increasing SSTs at 16.7 ka
 783 and again at ~ 14.7 ka (Davies et al., 2011). Alkenone-inferred paleo-SST reconstructions from
 784 this same core show the lowest SSTs ($\sim 5^\circ\text{C}$) circa 17.0 ka, with increased SSTs beginning ~ 16.5
 785 ka, and a rapid $\sim 3\text{--}4^\circ\text{C}$ rise in SSTs from 15.2 to 14.7 ka (Praetorius et al., 2015). Alkenone-
 786 inferred SST and $\delta^{18}\text{O}$ records from the Gulf of Alaska also record increased SSTs of $\sim 3^\circ\text{C}$ at
 787 14.7 ka (cores EW0408-26JC, EW0408-66JC; Praetorius et al., 2016). Off Vancouver Island,
 788 Mg/Ca temperature reconstructions from subsurface-dwelling *N. pachyderma* indicate two stages
 789 of warming of 2°C at 17.2 – 16 ka, and a further $\sim 3^\circ\text{C}$ 15.5 – 14.0 ka, while surface-dwelling
 790 *G. bulloides* record a 3°C SST increase from 15.0 – 14.0 ka (core MD02-2496; Taylor et al.,
 791 2014), all within the uncertainty of coastal Alexander Archipelago ice retreat. Alkenone SST
 792 reconstructions from another nearby core (core JT96-09) also indicates a 4°C increase in SST at
 793 ~ 14.7 ka (Kienast and McKay, 2001).

794 There are few terrestrial paleoclimate data that span the last deglacial period from
 795 [southeast Alaska](#) and coastal British Columbia. Cordilleran ice cover until ~ 15 ka across much of
 796 the region impeded the preservation of many terrestrial records – however, there are limited ice
 797 core, speleothem, and lake records that date back to early regional deglaciation or prior. A
 798 growth hiatus in a speleothem from El Capitan Cave (southern Alexander Archipelago) spanning
 799 ~ 41.5 to ~ 13.4 ka suggests the cave was either overridden by the [Cordilleran Ice Sheet](#),
 800 experienced permafrost conditions and a mean annual air temperature $< 0^\circ\text{C}$, or lacked drip
 801 water (Wilcox et al., 2019). [The youngest date also serves as a minimum limit on deglaciation, as](#)
 802 [the area was thawed by \$\sim 13.4\$ ka.](#) However, El Capitan Cave is ~ 60 km inland of the outermost
 803 coastal region and therefore may have still experienced these conditions while the outer coast
 804 deglaciated. At Hummingbird Lake, southwestern Baranof Island, pollen records indicate *Pinus*

Formatted: Normal, Right, Border: Top: (No border), Bottom: (No border), Left: (No border), Right: (No border), Between: (No border), Tab stops: 3.25", Centered + 6.5", Right, Position: Horizontal: Left, Relative to: Column, Vertical: In line, Relative to: Margin, Wrap Around

Formatted: Default Paragraph Font, Font: +Body (Calibri), Font color: Black

Formatted: Default Paragraph Font, Font: +Body (Calibri), Font color: Black

Formatted: Font: Calibri, Font color: Black

Deleted: -

Deleted: SE AK

Deleted: . Fisher et al. (2008) developed an ice core record from Mt. Logan, British Columbia. However, measurements of $\delta^{18}\text{O}$ likely represent shifting precipitation sources, rather than paleoclimate changes.

Deleted: CIS

812 *contorta* dominated from ~15.2 ka to 14 ka, which is interpreted to represent *Pinus contorta*
 813 response to the beginnings of Gulf of Alaska ocean warming at ~16.5 ka (Praetorius et al., 2015;
 814 Ager, 2019). This record suggests increased air temperatures around deglaciation of the
 815 Alexander Archipelago between 16.3 ± 0.8 ka and 15.1 ± 0.9 ka.

- Formatted: Default Paragraph Font, Font: +Body (Calibri), Font color: Black
- Formatted: Default Paragraph Font, Font: +Body (Calibri), Font color: Black
- Formatted: Normal, Right, Border: Top: (No border), Bottom: (No border), Left: (No border), Right: (No border), Between : (No border), Tab stops: 3.25", Centered + 6.5"; Right, Position: Horizontal: Left, Relative to: Column, Vertical: In line, Relative to: Margin, Wrap Around
- Formatted: Font: Calibri, Font color: Black

816 **5.6 Implications for early human migration**

817
 818 Several studies have [scrutinized](#) potential areas of [LLGM](#) glacial refugia in the Alexander
 819 Archipelago through a human migration perspective (Carrara et al., 2007; Lesnek et al., 2018),
 820 building off similar approaches from elsewhere in the North Pacific (e.g., Warner et al., 1982;
 821 Mann and Peteet, 1994; Misarti et al., 2012). Our study focused on southern Baranof and Kruzof
 822 islands because previous mapping suggested that parts of these areas were ice-free throughout
 823 the [LLGM](#) (Carrara et al., 2003; Carrara et al., 2007). However, our ¹⁰Be ages from southern
 824 Baranof Island indicate these areas were glaciated throughout the [LLGM](#) and not available for
 825 human habitation between ~20 ka and ~15.4 ka. Our exposure ages from Kruzof Island also
 826 suggest this area was not ice free until ~14.8 ka.

- Deleted: focused on scrutinizing
- Deleted: ILGM

827 These results indicate that some of the last major unevaluated areas of possible refugia
 828 presently above sea-level were covered by ice during the [LLGM](#). At its maximum extent, ice
 829 likely extended onto the then-exposed continental shelf. Ice occupation of the continental shelf –
 830 or at least parts of the shelf – off the Alexander Archipelago was relatively brief, from ~20.0 to
 831 ~16.0 ka (Lesnek et al., 2018). [Areas of the continental shelf](#) would have been above [modern](#) sea
 832 level during this time and until ~11 – 8 ka, when sea level neared modern levels in the Alexander
 833 Archipelago (Baichtal et al., [2021](#)). At a minimum, ice lobes would have existed within the
 834 major shelf troughs (e.g., Chatham Strait), likely [crossing](#) the entire shelf at these locations; at a
 835 maximum, the [entire](#) continental shelf may have been occupied by ice from ~20 to ~16 ka.

- Deleted: ILGM
- Deleted: ILGM
- Deleted:
- Deleted:
- Formatted: Font: +Body (Calibri), 11 pt
- Deleted: that
- Deleted:
- Deleted: that are
- Deleted: ILGM
- Deleted: Lowered global sea levels indicate
- Deleted: contemporary
- Deleted: in press
- Deleted:),
- Deleted: crossing
- Deleted: whole

857 Whether portions of the shelf remained ice-free during the [LLGM](#) is unknown, but it is possible.
 858 Based on the immediate colonization of *Pinus* at 15.2 ka in Hummingbird Lake, and as early as
 859 ~15.4 ka on Pleasant Island, there were likely ice-free areas on the shelf throughout the [LLGM](#)
 860 (Hansen and Engstrom, 1996; Ager, 2019).

861 **6 Conclusions**

862
 863 We conclude that several areas in [southeast Alaska](#) previously mapped as ice-free through the
 864 [LLGM](#) were covered by ice until between ~16.3 and ~15.1 ka. ¹⁰Be ages from boulders suggest
 865 that the northern coastal Alexander Archipelago deglaciated at 15.1 ± 0.9 ka, while ¹⁰Be and ³⁶Cl
 866 ages date ice retreat in the southern portion at 16.3 ± 0.8 ka, following a [LLGM](#) that began after
 867 ~20 ka (Lesnek et al., 2018; Lesnek et al., 2020) The timing of deglaciation in the Alexander
 868 Archipelago is similar to some other sites around the [Cordilleran Ice Sheet](#) coastal margin (e.g.,
 869 Mann and Peteet, 1994; Misarti et al., 2012), but later than other locations (e.g., Darvill et al.,
 870 2018). Notably, the deglaciation in [southeast Alaska](#) is later than in mainland Alaska and Kodiak
 871 and Sanak Islands, Alaska ([Fig. 1](#)), where records are more aligned with the [GLGM](#). The timing
 872 of deglaciation in the Alexander Archipelago is broadly synchronous with regional records of
 873 local ocean and air temperature increases. We also found that anomalously old ¹⁰Be ages of
 874 bedrock surfaces are [likely](#) due to inheritance caused by insufficient ice sheet erosion, and thus,
 875 [urge](#) caution [when](#) using ages from bedrock surfaces as direct constraints on ice retreat without
 876 additional boulder ages along the coastal margins of the [Cordilleran Ice Sheet](#).

877 Our data indicate that previous mapping of the coastal [Cordilleran Ice Sheet](#) can be
 878 spatially and temporally improved. We suggest that ice likely extended out on the continental
 879 shelf along the Alexander Archipelago. We are increasingly confident that areas of the coastal
 880 [Cordilleran Ice Sheet](#) previously mapped as ice-free throughout the [LLGM](#) were in fact covered

Formatted: Normal, Right, Border: Top: (No border), Bottom: (No border), Left: (No border), Right: (No border), Between: (No border), Tab stops: 3.25", Centered + 6.5", Right, Position: Horizontal: Left, Relative to: Column, Vertical: In line, Relative to: Margin, Wrap Around

Formatted: Default Paragraph Font, Font: +Body (Calibri), Font color: Black

Formatted: Default Paragraph Font, Font: +Body (Calibri), Font color: Black

Formatted: Font: Calibri, Font color: Black

Deleted: ILGM

Deleted: ,

Deleted: ILGM

Deleted: SE AK

Deleted: ILGM

Deleted: ,

Deleted:

Deleted: ILGM

Deleted: begin

Deleted: CIS

Deleted: SE AK

Deleted: ,

Deleted: gLGM

Deleted: , we

Deleted: CIS

Deleted: CIS

Deleted: CIS

Deleted: ILGM

899 by ice, and that refugia, if any existed, would have been located on the exposed continental shelf.

900 Although more logistically challenging, subsequent studies should evaluate the existence of

901 LLGM refugia in the Alexander Archipelago by focusing on the previously exposed continental

902 shelf. Special attention should be given to the northern Alexander Archipelago where ice masses

903 were fed by local ice caps and thus may not have been as extensive, as opposed to elsewhere in

904 the northeastern Pacific where ice was sourced from the main body of the Cordilleran Ice Sheet.

905
906

907 **7 Acknowledgements**

908 We acknowledge that these samples were collected on the ancestral lands of the Tlingit and that
909 the University at Buffalo exists on the land of the Seneca. These peoples are the traditional
910 caretakers of these lands and we give thanks for the opportunity to exist and work on lands that
911 are rightfully theirs. We thank the Tongass National Forest for assistance with permitting and
912 logistics. We thank Corey Krabbenhoft, Joseph Tulenko and Karlee Prince for field assistance
913 and Joseph Tulenko and Chris Sbarra for lab assistance. We also thank PRIME Lab for ¹⁰Be
914 measurements and Lawrence Livermore National Laboratory for ³⁶Cl measurements. This
915 research was funded by NSF (award # 1854550), the National Geographic Society (award #
916 57989R-19), a Geological Society of America Student Research Grant (grant number 13631)
917 funded by NSF (award # 1949901), the Alaska Geological Society, and the Mark Diamond
918 Research Fund of the Graduate Student Association at the University at Buffalo, the State
919 University of New York.
920

921 **8. Author Contributions**

Formatted: Normal, Right, Border: Top: (No border), Bottom: (No border), Left: (No border), Right: (No border), Between : (No border), Tab stops: 3.25", Centered + 6.5", Right, Position: Horizontal: Left, Relative to: Column, Vertical: In line, Relative to: Margin, Wrap Around

Formatted: Default Paragraph Font, Font: +Body (Calibri), Font color: Black

Formatted: Default Paragraph Font, Font: +Body (Calibri), Font color: Black

Formatted: Font: Calibri, Font color: Black

Deleted: ILGM

Deleted: CIS.

Formatted: Heading 1, Indent: First line: 0", Line spacing: single

Formatted: Normal

Deleted: ¶
¶
¶
¶
8

930 [JPB designed the study framework and acquired the majority of grant funds. CKW acquired](#)
 931 [supplementary funding for fieldwork and lab analyses. CKW, JPB, JFB, and AJL collected](#)
 932 [samples in the field. CKW conducted 10Be work and AJL and JML performed 36Cl chemistry.](#)
 933 [CKW, JPB, AJL, and JML analyzed sample data and calculated ages. All authors were involved](#)
 934 [in interpreting the data. CKW wrote the first draft of the manuscript; all authors provided](#)
 935 [substantial input. CKW and AJL created figures and tables.](#)

936

937 [9](#) References

938

939 Addison, J. A., Beget, J. E., Ager, T. A., and Finney, B. P.: Marine tephrochronology of the Mt.
 940 Edgumbe volcanic field, southeast Alaska, USA, *Quaternary Research*, 73, 277-292,
 941 2010.

942 Ager, T. A.: Late Quaternary vegetation development following deglaciation of northwestern
 943 Alexander Archipelago, Alaska, *Frontiers in Earth Science*, 7, 104, 2019.

944 Baichtal, J. F., Lesnek, A. J., Carlson, R. J., Schmuck, N., Smith, J. L., Landwehr, D. J., and
 945 Briner, J. P.: Late Pleistocene and Early Holocene Sea level History Glacial Retreat
 946 Interpreted from Shell-bearing Marine Deposits of Southeastern Alaska, *GSA Geosphere*,
 947 [2021](#).

948 Balco, G., Stone, J. O., Lifton, N. A., and Dunai, T. J.: A complete and easily accessible means
 949 of calculating surface exposure ages or erosion rates from 10Be and 26Al measurements,
 950 *Quaternary Geochronology*, 3, 174-195, <https://doi.org/10.1016/j.quageo.2007.12.001>,
 951 2008.

952 Balco, G.: Production rate calculations for cosmic-ray-muon-produced 10Be and 26Al
 953 benchmarked against geological calibration data, *Quaternary Geochronology*, 39, 150-
 954 173, 2017.

955 Barrie, J. V., and Conway, K. W.: Late Quaternary glaciation and postglacial stratigraphy of the
 956 northern Pacific margin of Canada, *Quaternary Research*, 51, 113-123, 1999.

957 Begét, J. E., and Motyka, R. J.: New dates on late Pleistocene dacitic tephra from the Mount
 958 Edgumbe volcanic field, southeastern Alaska, *Quaternary Research*, 49, 123-125, 1998.

959 Blaise, B., Clague, J. J., and Mathewes, R. W.: Time of maximum Late Wisconsin glaciation,
 960 West Coast of Canada, *Quaternary Research*, 34, 282-295, [https://doi.org/10.1016/0033-5894\(90\)90041-I](https://doi.org/10.1016/0033-5894(90)90041-I), 1990.

962 Booth, D. B., Troost, K. G., Clague, J. J., and Waitt, R. B.: The Cordilleran ice sheet,
 963 *Developments in Quaternary Sciences*, 1, 17-43, 2003.

964 Borchers, B., Marrero, S., Balco, G., Caffee, M., Goehring, B., Lifton, N., Nishiizumi, K.,
 965 Phillips, F., Schaefer, J., and Stone, J. J. Q. G.: Geological calibration of spallation
 966 production rates in the CRONUS-Earth project, 31, 188-198, 2016.

967 Brew, David A.: Geologic map of the Craig, Dixon Entrance, and parts of the Ketchikan and
 968 Prince Rupert quadrangles, Southeastern Alaska, No. 95-215, 1995.

Formatted: Default Paragraph Font, Font: +Body (Calibri),
 Font color: Black

Formatted: Default Paragraph Font, Font: +Body (Calibri),
 Font color: Black

Formatted: Normal, Right, Border: Top: (No border),
 Bottom: (No border), Left: (No border), Right: (No border),
 Between : (No border), Tab stops: 3.25", Centered + 6.5",
 Right, Position: Horizontal: Left, Relative to: Column,
 Vertical: In line, Relative to: Margin, Wrap Around

Formatted: Font: Calibri, Font color: Black

Deleted: in press

Deleted: James

Deleted: .,

Deleted: Roman J.

Deleted: . "

Deleted: . "

Deleted: .1 (1998):

- 976 Briner, J. P., and Swanson, T. W.: Using inherited cosmogenic ^{36}Cl to constrain glacial erosion
 977 rates of the Cordilleran ice sheet, *Geology*, 26, 3-6, 1998.
- 978 [Briner, J. P., Goehring, B. M., Mangerud, J., and Svendsen, J. I.: The deep accumulation of \$^{10}\text{Be}\$
 979 at Utsira, southwestern Norway: implications for cosmogenic nuclide exposure dating in
 980 peripheral ice sheet landscapes, *Geophysical Research Letters*, 43, 9121-9129, 2016.](#)
- 981 Briner, J. P., Tulenko, J. P., Kaufman, D. S., Young, N. E., Baichtal, J. F., and Lesnek, A.: The
 982 last deglaciation of Alaska, *Cuadernos de investigación geográfica/Geographical*
 983 *Research Letters*, 429-448, 2017.
- 984 Caissie, B. E., Brigham-Grette, J., Lawrence, K. T., Herbert, T. D., and Cook, M. S.: Last Glacial
 985 Maximum to Holocene sea surface conditions at Umnak Plateau, Bering Sea, as inferred
 986 from diatom, alkenone, and stable isotope records, *Paleoceanography*, 25, 2010.
- 987 Capps, S. R.: Glaciation in [Alaska](#), 2330-7102, 1932.
- 988 Carrara, P. E., Ager, T. A., Baichtal, J. F., and VanSistine, D. P.: Map of glacial limits and
 989 possible refugia in the southern Alexander Archipelago, Alaska, during the late
 990 Wisconsin glaciation, Report 2424, 2003.
- 991 Carrara, P. E., Ager, T. A., and Baichtal, J. F.: Possible refugia in the Alexander Archipelago of
 992 southeastern Alaska during the late Wisconsin glaciation, *Canadian Journal of Earth*
 993 *Sciences*, 44, 229-244, 10.1139/e06-081, 2007.
- 994
- 995 Cook, J. A., Bidlack, A. L., Conroy, C. J., Demboski, J. R., Fleming, M. A., Runck, A. M.,
 996 Stone, K. D., and MacDonald, S. O.: A phylogeographic perspective on endemism in the
 997 Alexander Archipelago of southeast Alaska, *Biological Conservation*, 97, 215-227,
 998 [https://doi.org/10.1016/S0006-3207\(00\)00114-2](https://doi.org/10.1016/S0006-3207(00)00114-2), 2001.
- 999 Corbett, L. B., Bierman, P. R., and Rood, D. H.: An approach for optimizing in situ cosmogenic
 1000 ^{10}Be sample preparation, *Quaternary Geochronology*, 33, 24-34,
 1001 <https://doi.org/10.1016/j.quageo.2016.02.001>, 2016.
- 1002 Cosma, T. N., Hendy, I. L., and Chang, A. S.: Chronological constraints on Cordilleran Ice Sheet
 1003 glaciomarine sedimentation from core MD02-2496 off Vancouver Island (western
 1004 Canada), *Quaternary Science Reviews*, 27, 941-955,
 1005 <https://doi.org/10.1016/j.quascirev.2008.01.013>, 2008.
- 1006 Dalton, A. S., Margold, M., Stokes, C. R., Tarasov, L., Dyke, A. S., Adams, R. S., Allard, S.,
 1007 Arends, H. E., Atkinson, N., and Attig, J. W.: An updated radiocarbon-based ice margin
 1008 chronology for the last deglaciation of the North American Ice Sheet Complex,
 1009 *Quaternary Science Reviews*, 234, 106223, 2020.
- 1010 Darvill, C. M., Menounos, B., Goehring, B. M., Lian, O. B., and Caffee, M. W.: Retreat of the
 1011 western Cordilleran ice sheet margin during the last deglaciation, *Geophysical Research*
 1012 *Letters*, 45, 9710-9720, 2018.
- 1013 Davies, M. H., Mix, A. C., Stoner, J. S., Addison, J. A., Jaeger, J., Finney, B., and Wiest, J.: The
 1014 deglacial transition on the southeastern Alaska Margin: Meltwater input, sea level rise,
 1015 marine productivity, and sedimentary anoxia, *Palaeogeography and Palaeoclimatology*,
 1016 26, 10.1029/2010pa002051, 2011.
- 1017 Demboski, J. R., Stone, K. D., and Cook, J. A.: [Further perspectives on the Haida Gwaii glacial
 1018 refugium](#), *Evolution*, 53, 2008-2012, 10.1111/j.1558-5646.1999.tb04584.x, 1999.
- 1019 Dyke, A. S.: An outline of North American deglaciation with emphasis on central and northern
 1020 Canada, *Developments in quaternary sciences*, 2, 373-424, 2004.

Formatted: Normal, Right, Border: Top: (No border), Bottom: (No border), Left: (No border), Right: (No border), Between: (No border), Tab stops: 3.25", Centered + 6.5", Right, Position: Horizontal: Left, Relative to: Column, Vertical: In line, Relative to: Margin, Wrap Around

Formatted: Default Paragraph Font, Font: +Body (Calibri), Font color: Black

Formatted: Default Paragraph Font, Font: +Body (Calibri), Font color: Black

Formatted: Font: Calibri, Font color: Black

Deleted: -

Deleted: Alaska2330

Deleted: Clague, J. J., Armstrong, J. E., and Mathews, W. H.: Advance of the late Wisconsin Cordilleran Ice Sheet in southern British Columbia since 22,000 Yr B.P., *Quaternary Research*, 13, 322-326, [https://doi.org/10.1016/0033-5894\(80\)90060-5](https://doi.org/10.1016/0033-5894(80)90060-5), 1980.

Deleted: A.: FURTHER PERSPECTIVES ON THE HAIDA GWAII GLACIAL REFUGIUM

- 1030 Eberlein, G. D., Churkin, M., Carter, C., Berg, H., and Ovenshine, A.: Geology of the Craig
1031 quadrangle, Alaska, US Geological Survey, 2331-1258, 1983.
- 1032 [Faure, G.: Isotope systematics in two-component mixtures, Principles of isotope geology, 141-
1033 153, 1986.](#)
- 1034 [Gosse, J. C., and Phillips, F. M.: Terrestrial in situ cosmogenic nuclides: theory and application,
1035 Quaternary Science Reviews, 20, 1475-1560, 2001.](#)
- 1036 Gregoire, L. J., Otto-Bliesner, B., Valdes, P. J., and Ivanovic, R.: Abrupt Bølling warming and
1037 ice saddle collapse contributions to the Meltwater Pulse 1a rapid sea level rise,
1038 Geophysical research letters, 43, 9130-9137, 2016.
- 1039 Hansen, B. C. S., and Engstrom, D. R.: Vegetation history of Pleasant Island, southeastern
1040 Alaska, since 13,000 yr BP, Quaternary Research, 46, 161-175, 1996.
- 1041 [Hebda, C. F. G., McLaren, D., Mackie, O., Fedje, D., Pedersen, M. W., Willerslev, E., Brown,
1042 K.,
1043 J., and Hebda, R. J.: Late Pleistocene palaeoenvironments and a possible glacial refugium
1044 on northern Vancouver Island, Canada: Evidence for the viability of early human
1045 settlement on the northwest coast of North America, Quaternary Science Reviews, 279,
1046 107388, 2022.](#)
- 1047 Ivanovic, R. F., Gregoire, L. J., Wickert, A. D., Valdes, P. J., and Burke, A.: Collapse of the
1048 North American ice saddle 14,500 years ago caused widespread cooling and reduced
1049 ocean overturning circulation, Geophysical Research Letters, 44, 383-392, 2017.
- 1050 Jones, R. S., Whitehouse, P. L., Bentley, M. J., Small, D., and Dalton, A. S.: Impact of glacial
1051 isostatic adjustment on cosmogenic surface-exposure dating, Quaternary Science
1052 Reviews, 212, 206-212, 2019.
- 1053 Kienast, S. S., and McKay, J. L.: Sea surface temperatures in the subarctic northeast Pacific
1054 reflect millennial-scale climate oscillations during the last 16 kyrs, Geophysical Research
1055 Letters, 28, 1563-1566, 2001.
- 1056 Lal, D.: Cosmic ray labeling of erosion surfaces: in situ nuclide production rates and erosion
1057 models, Earth and Planetary Science Letters, 104, 424-439, 1991.
- 1058 Lesnek, A. J., Briner, J. P., Lindqvist, C., Baichtal, J. F., and Heaton, T. H.: Deglaciation of the
1059 Pacific coastal corridor directly preceded the human colonization of the Americas,
1060 Science Advances, 4, 2018.
- 1061 Lesnek, A. J., Briner, J. P., Baichtal, J. F., and Lyles, A. S.: New constraints on the last
1062 deglaciation of the Cordilleran Ice Sheet in coastal Southeast Alaska, Quaternary
1063 Research, 96, 140-160, 2020.
- 1064 Maier, E., Zhang, X., Abelman, A., Gersonde, R., Mulitza, S., Werner, M., Méheust, M., Ren,
1065 J., Chaplign, B., and Meyer, H.: North Pacific freshwater events linked to changes in
1066 glacial ocean circulation, Nature, 559, 241-245, 2018.
- 1067 Mann, D. H.: Wisconsin and Holocene glaciation of southeast Alaska, 1986.
- 1068 Mann, D. H., and Peteet, D. M.: Extent and Timing of the Last Glacial Maximum in
1069 Southwestern Alaska, Quaternary Research, 42, 136-148,
1070 <https://doi.org/10.1006/qres.1994.1063>, 1994.
- 1071 Mann, D. H., and Hamilton, T. D.: Late Pleistocene and Holocene Paleoenvironments of the
1072 Pacific Coast, Quaternary Science Reviews, 14, 449-471, 10.1016/0277-3791(95)00016-
1073 i, 1995.
- 1074 [Marrero, S.M., Phillips, F.M., Caffee, M.W. and Gosse, J.C.: CRONUS-Earth cosmogenic ³⁶Cl
1075 calibration. Quaternary Geochronology, 31, 199-219, 2016.](#)

Formatted: Default Paragraph Font, Font: +Body (Calibri),
Font color: Black

Formatted: Default Paragraph Font, Font: +Body (Calibri),
Font color: Black

Formatted: Normal, Right, Border: Top: (No border),
Bottom: (No border), Left: (No border), Right: (No border),
Between : (No border), Tab stops: 3.25", Centered + 6.5";
Right, Position: Horizontal: Left, Relative to: Column,
Vertical: In line, Relative to: Margin, Wrap Around

Formatted: Font: Calibri, Font color: Black

Deleted: Fisher, D., Osterberg, E., Dyke, A., Dahl-Jensen,
D., Demuth, M., Zdanowicz,

Moved down [2]: C.,

Deleted: Bourgeois, J., Koerner, R. M., Mayewski, P., and
Wake, C.: The Mt Logan Holocene—late Wisconsinan
isotope record: tropical Pacific—Yukon connections, The
Holocene, 18, 667-677, 2008.¶

Moved (insertion) [2]

Deleted: -

Deleted: eaar5040, 10.1126/sciadv.aar5040 %J Science
Advances, 2018....

Deleted: Marrero, S

Moved down [3]: . M.,

Deleted: Phillips, F. M., Borchers, B., Lifton, N., Aumer,
R. and Balco, G: Cosmogenic nuclide systematics and the
CRONUScale program, Quaternary Geochronology, 31,
160-187, 2016a.¶

Deleted: 2016b

- 1093 [Menounos, B., Goehring, B. M., Osborn, G., Margold, M., Ward, B., Bond, J., Clarke, G. K. C.,](#)
 1094 [Clague, J. J., Lakeman, T., Koch, J., Caffee, M. W., Gosse, J., Stroeven, A. P., Seguinot,](#)
 1095 [J., and Heyman, J.: Cordilleran Ice Sheet mass loss preceded climate reversals near the](#)
 1096 [Pleistocene Termination, *Science*, 358, 781, 10.1126/science.aan3001, 2017.](#)
- 1097 Mathewes, R. W., and Clague, J. J.: Paleocology and ice limits of the early Fraser glaciation
 1098 (Marine Isotope Stage 2) on Haida Gwaii, British Columbia, Canada, *Quaternary*
 1099 *Research*, 88, 277-292, 10.1017/qua.2017.36, 2017.
- 1100 Miller, R. D.: Gastineau channel formation: a composite glaciomarine deposit near Juneau,
 1101 Alaska, US Government Printing Office, 1973.
- 1102 Misarti, N., Finney, B. P., Jordan, J. W., Maschner, H. D. G., Addison, J. A., Shapley, M. D.,
 1103 Krumhardt, A., and Beget, J. E.: Early retreat of the Alaska Peninsula Glacier Complex
 1104 and the implications for coastal migrations of First Americans, *Quaternary Science*
 1105 *Reviews*, 48, 1-6, <https://doi.org/10.1016/j.quascirev.2012.05.014>, 2012.
- 1106 Molnia, B. F.: *Glaciers of North America-Glaciers of Alaska*, Geological Survey (US), 2008.
- 1107 Nishiizumi, K., Imamura, M., Caffee, M. W., Southon, J. R., Finkel, R. C., and McAninch, J.:
 1108 Absolute calibration of ¹⁰Be AMS standards, *Nuclear Instruments and Methods in*
 1109 *Physics Research Section B: Beam Interactions with Materials and Atoms*, 258, 403-413,
 1110 <https://doi.org/10.1016/j.nimb.2007.01.297>, 2007.
- 1111 Porter, S. C., and Swanson, T. W.: Radiocarbon age constraints on rates of advance and retreat of
 1112 the Puget lobe of the Cordilleran ice sheet during the last glaciation, *Quaternary*
 1113 *Research*, 50, 205-213, 1998.
- 1114 Praetorius, S., Mix, A., Jensen, B., Froese, D., Milne, G., Wolhowe, M., Addison, J., and Prahll,
 1115 F.: Interaction between climate, volcanism, and isostatic rebound in Southeast Alaska
 1116 during the last deglaciation, *Earth and Planetary Science Letters*, 452, 79-89, 2016.
- 1117 Praetorius, S. K., and Mix, A. C.: Synchronization of North Pacific and Greenland climates
 1118 preceded abrupt deglacial warming, *Science*, 345, 444-448, 2014.
- 1119 Praetorius, S. K., Mix, A. C., Walczak, M. H., Wolhowe, M. D., Addison, J. A., and Prahll, F. G.:
 1120 North Pacific deglacial hypoxic events linked to abrupt ocean warming, *Nature*, 527,
 1121 362-366, 2015.
- 1122 Reger, R. D., Pinney, D. S., Burke, R. M., and Wiltse, M. A.: Catalog and initial analyses of
 1123 geologic data related to middle to late Quaternary deposits, Cook Inlet region, Alaska,
 1124 State of Alaska Division of Geological and Geophysical Surveys Report of
 1125 Investigations, 95-96, 1996.
- 1126 Riehle, J. R., Brew, D. A., Reed, K. M., and Bartsch-Winkler, S.: Explosive latest Pleistocene (?)
 1127 and Holocene activity of the Mount Edgecumbe volcanic field, Alaska, *US Geological*
 1128 *Survey Circular*, 939, 111-114, 1984.
- 1129 Riehle, J. R., Champion, D. E., Brew, D. A., and Lanphere, M. A.: Pyroclastic deposits of the
 1130 Mount Edgecumbe volcanic field, southeast Alaska: eruptions of a stratified magma
 1131 chamber, *Journal of volcanology and geothermal research*, 53, 117-143, 1992.
- 1132 Riehle, J. R.: *The Mount Edgecumbe Volcanic Field: A Geologic History*, US Department of
 1133 Agriculture, Forest Service, Alaska Region, 1996.
- 1134 Seguinot, J., Khroulev, C., Rogozhina, I., Stroeven, A. P., and Zhang, Q.: The effect of climate
 1135 forcing on numerical simulations of the Cordilleran ice sheet at the Last Glacial
 1136 Maximum, *The Cryosphere*, 8, 1087-1103, 2014.

Formatted: Default Paragraph Font, Font: +Body (Calibri),
 Font color: Black

Formatted: Normal, Right, Border: Top: (No border),
 Bottom: (No border), Left: (No border), Right: (No border),
 Between : (No border), Tab stops: 3.25", Centered + 6.5",
 Right, Position: Horizontal: Left, Relative to: Column,
 Vertical: In line, Relative to: Margin, Wrap Around

Formatted: Default Paragraph Font, Font: +Body (Calibri),
 Font color: Black

Formatted: Font: Calibri, Font color: Black

Moved (insertion) [3]

- 1137 Seguinot, J., Rogozhina, I., Stroeven, A. P., Margold, M., and Kleman, J.: Numerical simulations
 1138 of the Cordilleran ice sheet through the last glacial cycle, *The Cryosphere*, 10, 639-664,
 1139 2016.
- 1140 Shafer, A. B., Cullingham, C. I., Cote, S. D., and Coltman, D. W.: Of glaciers and refugia: a
 1141 decade of study sheds new light on the phylogeography of northwestern North America,
 1142 *Mol Ecol*, 19, 4589-4621, 10.1111/j.1365-294X.2010.04828.x, 2010.
- 1143 Shafer, A. B. A., White, K. S., Côté, S. D., and Coltman, D. W.: Deciphering translocations from
 1144 relicts in Baranof Island mountain goats: is an endemic genetic lineage at risk?,
 1145 *Conservation Genetics*, 12, 1261-1268, 10.1007/s10592-011-0227-8, 2011.
- 1146 Shakun, J. D., Clark, P. U., He, F., Marcott, S. A., Mix, A. C., Liu, Z., Otto-Bliesner, B.,
 1147 Schmittner, A., and Bard, E.: Global warming preceded by increasing carbon dioxide
 1148 concentrations during the last deglaciation, *Nature*, 484, 49-54, 2012.
- 1149 Spratt, R. M., and Lisiecki, L. E.: A Late Pleistocene sea level stack, *Climate of the Past*, 12,
 1150 1079-1092, 2016.
- 1151 Staiger, J., Gosse, J., Toracinta, R., Oglesby, B., Fastook, J., and Johnson, J. V.: Atmospheric
 1152 scaling of cosmogenic nuclide production: climate effect, *Journal of Geophysical
 1153 Research: Solid Earth*, 112, 2007.
- 1154 Stuiver, M., Reimer, P.J., and Reimer, R.W., CALIB 8.2, <http://calib.org>, 2021.
- 1155 Tarasov, L., Dyke, A. S., Neal, R. M., and Peltier, W. R.: A data-calibrated distribution of
 1156 deglacial chronologies for the North American ice complex from glaciological modeling,
 1157 *Earth and Planetary Science Letters*, 315-316, 30-40,
 1158 <https://doi.org/10.1016/j.epsl.2011.09.010>, 2012.
- 1159 Taylor, M. A., Hendy, I. L., and Pak, D. K.: Deglacial ocean warming and marine margin retreat
 1160 of the Cordilleran Ice Sheet in the North Pacific Ocean, *Earth and Planetary Science
 1161 Letters*, 403, 89-98, 10.1016/j.epsl.2014.06.026, 2014.
- 1162 Warner, B. G., Mathewes, R. W., and Clague, J. J.: Ice-free conditions on the Queen Charlotte
 1163 Islands, British Columbia, at the height of late Wisconsin glaciation, *Science*, 218, 675-
 1164 677, 1982.
- 1165 Wilcox, P. S., Dorale, J. A., Baichtal, J. F., Spotl, C., Fowell, S. J., Edwards, R. L., and Kovarik,
 1166 J. L.: Millennial-scale glacial climate variability in Southeastern Alaska follows
 1167 Dansgaard-Oeschger cyclicality, *Sci Rep*, 9, 7880, 10.1038/s41598-019-44231-1, 2019.
- 1168 Wilson, F. H., Hults, C. P., Mull, C. G., and Karl, S. M.: Geologic map of Alaska, US
 1169 Department of the Interior, US Geological Survey, 2015.
- 1170 Young, N. E., Schaefer, J. M., Briner, J. P., and Goehring, B. M.: A ^{10}Be production-rate
 1171 calibration for the Arctic, *Journal of Quaternary Science*, 28, 515-526, 2013.

Formatted: Default Paragraph Font, Font: +Body (Calibri),
Font color: Black

Formatted: Normal, Right, Border: Top: (No border),
Bottom: (No border), Left: (No border), Right: (No border),
Between : (No border), Tab stops: 3.25", Centered + 6.5",
Right, Position: Horizontal: Left, Relative to: Column,
Vertical: In line, Relative to: Margin, Wrap Around

Formatted: Default Paragraph Font, Font: +Body (Calibri),
Font color: Black

Formatted: Font: Calibri, Font color: Black

Field Code Changed

Formatted: Default Paragraph Font, Font: +Body (Calibri),
11 pt, Font color: Custom Color(RGB(5,99,193))

1172

1173

1174

1175

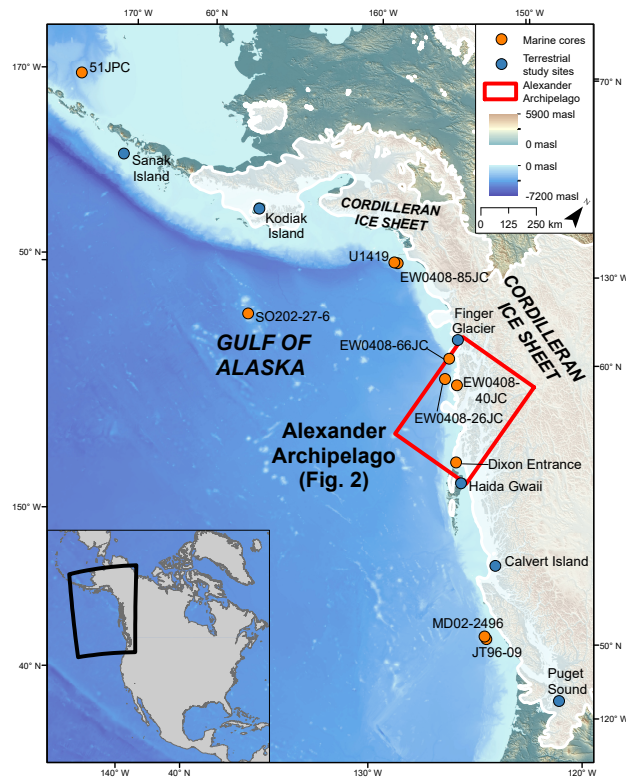
1176

1177

1178

1179
1180
1181
1182

1183 **Figures**



1184

1185 Figure 1: Map of the north Pacific region showing ice limits at 18.0 ka from Dalton et al. (2020)
 1186 with location of relevant sites mentioned in the text. The Alexander Archipelago is highlighted
 1187 by the red box, on the main figure. Orange dots indicate locations of marine sediment cores: 51-
 1188 JPC (Caissie et al., 2010), SO202-27-6 (Maier et al., 2018), U1419 (Walczak et al., 2020),
 1189 EW0408-85JC (Davies et al., 2011; Praetorius and Mix, 2014, Praetorius et al., 2015), EW0408-

31

Formatted: Default Paragraph Font, Font: +Body (Calibri), Font color: Black

Formatted: Default Paragraph Font, Font: +Body (Calibri), Font color: Black

Formatted: Normal, Right, Border: Top: (No border), Bottom: (No border), Left: (No border), Right: (No border), Between : (No border), Tab stops: 3.25", Centered + 6.5", Right, Position: Horizontal: Left, Relative to: Column, Vertical: In line, Relative to: Margin, Wrap Around

Formatted: Font: Calibri, Font color: Black

Deleted: ¶
¶
¶
¶
¶
¶

Formatted: Font: Times New Roman, Bold

Deleted: ¶ ... [2]

Formatted: Font color: Auto

Formatted: Space Before: 12 pt, After: 12 pt

Formatted: Font: 11 pt, Font color: Auto

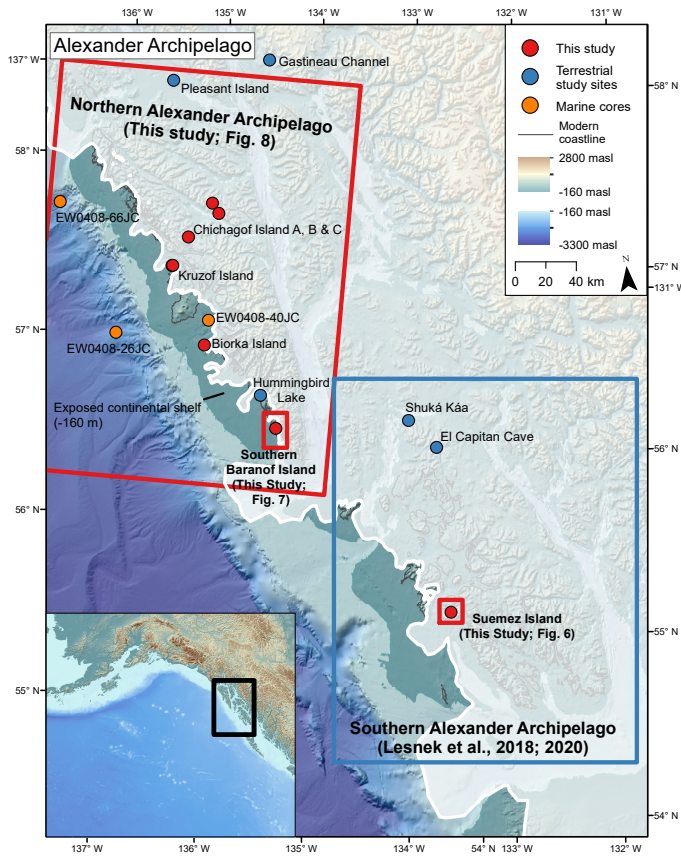
Formatted: Font color: Auto

Deleted: .

Formatted: Font color: Auto

Formatted: Font color: Auto

1202 66JC (Praetorius and Mix, 2014; Praetorius et al., 2016), EW0408-26JC (Praetorius and Mix,
 1203 2014; Praetorius et al., 2016), EW0408-40JC (Addison et al., 2010), MD02-2496 (Cosma and
 1204 Hendy, 2008), and JT96-09 (Kienast and McKay, 2001). Blue dots indicate location of terrestrial
 1205 study sites: Sanak Island (Misarti et al., 2012), Kodiak Island (Mann and Peteet, 1994), Finger
 1206 Glacier (Mann 1986), Haida Gwaii (Clague et al., 1982; Mathewes and Clague, 1982), Calvert
 1207 Island, (Darvill et al., 2018), and Puget Sound (Porter and Swanson, 1998).



1208 Figure 2: The Alexander Archipelago showing relevant marine sediment cores and terrestrial
 1209 chronologies. Shaded white areas show hypothesized [LLGM Cordilleran Ice Sheet](#) extent
 1210 (Lesnek et al., 2020). -160 m relative sea level lowering after Baichtal et al. (2021). Red boxes
 1212

32

Formatted: Normal, Right, Border: Top: (No border), Bottom: (No border), Left: (No border), Right: (No border), Between: (No border), Tab stops: 3.25", Centered + 6.5", Right, Position: Horizontal: Left, Relative to: Column, Vertical: In line, Relative to: Margin, Wrap Around

Formatted: Default Paragraph Font, Font: +Body (Calibri), Font color: Black

Formatted: Default Paragraph Font, Font: +Body (Calibri), Font color: Black

Formatted: Font: Calibri, Font color: Black

Deleted: Mt. Logan (Fisher et al., 2008),

Formatted: Font color: Auto

Deleted: Coquitlam Valley (Clague et al., 1980),

Formatted: Font color: Auto

Deleted: [...](#) [3]

Formatted: Font color: Auto

Formatted: Space After: 8 pt, Line spacing: Multiple 1.08 li, Left Horizontal

Formatted: Font: Bold, Font color: Auto

Formatted: Font color: Auto

Deleted: ILGM CIS

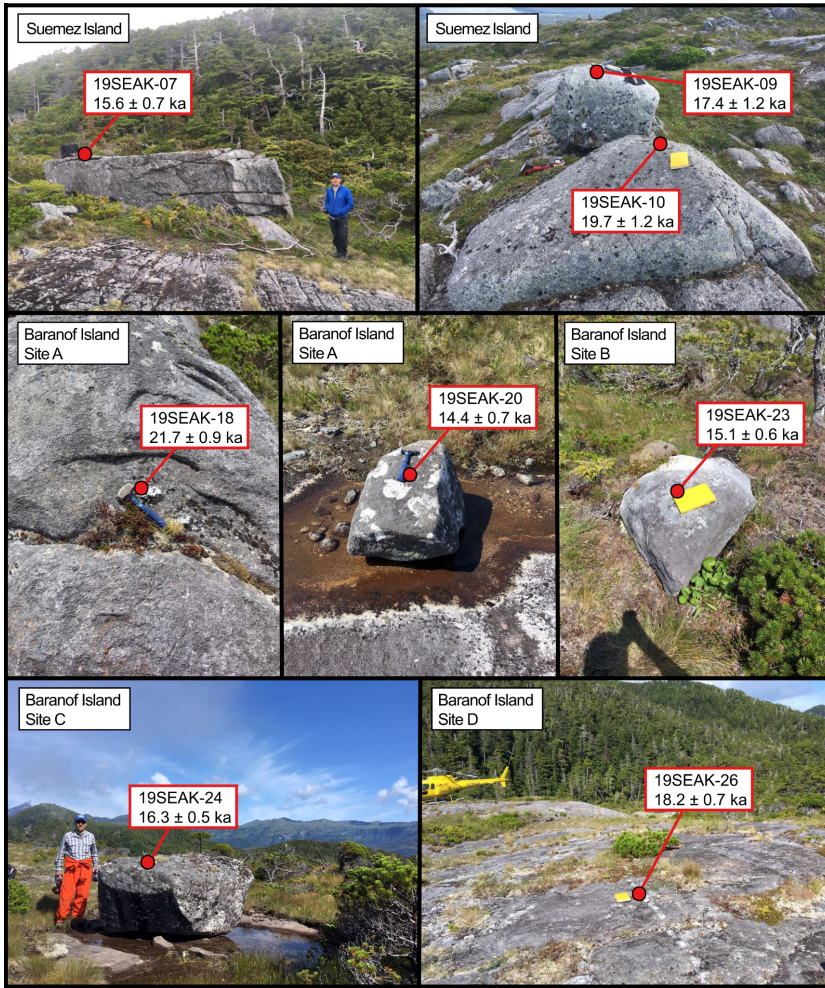
Formatted: Font color: Auto

Formatted: Font color: Auto

Deleted: in press

Formatted: Font color: Auto

1221 and points show sampling locations from this study. Blue box shows extent of study area from
 1222 Lesnek et al. (2018; 2020). Orange dots represent locations of marine sediment cores: EW0408-
 1223 66JC and EW0408-26J (Praetorius and Mix, 2014; Praetorius et al., 2016) and EW0408-40JC
 1224 (Addison et al., 2010). Blue dots indicate locations of relevant terrestrial study sites: Gastineau
 1225 Channel (Miller, 1973), Pleasant Island (Hansen and Engstrom, 1996), Hummingbird Lake
 1226 (Ager, 2019), [Shuká Káa](#) (Lesnek et al., 2018), and El Capitan Cave (Wilcox et al., 2019).



33

Formatted: Default Paragraph Font, Font: +Body (Calibri), Font color: Black

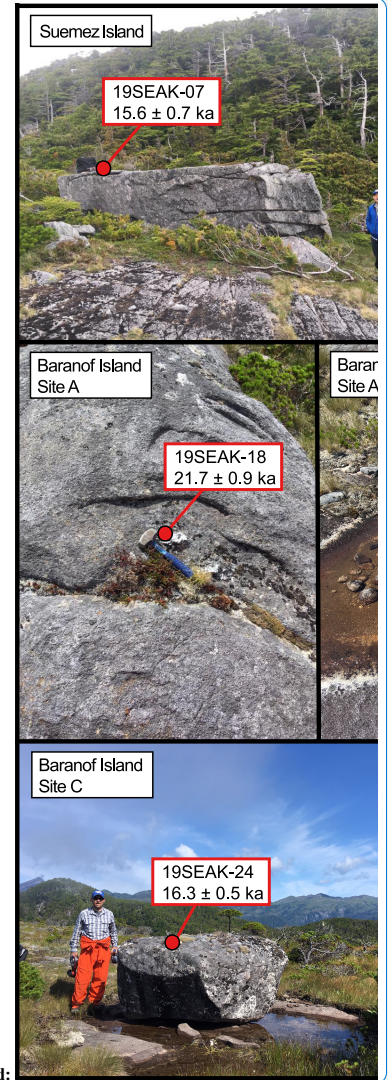
Formatted: Default Paragraph Font, Font: +Body (Calibri), Font color: Black

Formatted: Normal, Right, Border: Top: (No border), Bottom: (No border), Left: (No border), Right: (No border), Between : (No border), Tab stops: 3.25", Centered + 6.5", Right, Position: Horizontal: Left, Relative to: Column, Vertical: In line, Relative to: Margin, Wrap Around

Formatted: Font: Calibri, Font color: Black

Deleted: Shuká Káa

Formatted ... [4]



1227
1228

Figure 3: Sample photos from 2019 field season. All ^{10}Be ages shown with 1σ internal uncertainty.



34

Formatted: Default Paragraph Font, Font: +Body (Calibri), Font color: Black

Formatted: Default Paragraph Font, Font: +Body (Calibri), Font color: Black

Formatted: Normal, Right, Border: Top: (No border), Bottom: (No border), Left: (No border), Right: (No border), Between: (No border), Tab stops: 3.25", Centered + 6.5", Right, Position: Horizontal: Left, Relative to: Column, Vertical: In line, Relative to: Margin, Wrap Around

Formatted: Font: Calibri, Font color: Black

Formatted: Font color: Auto

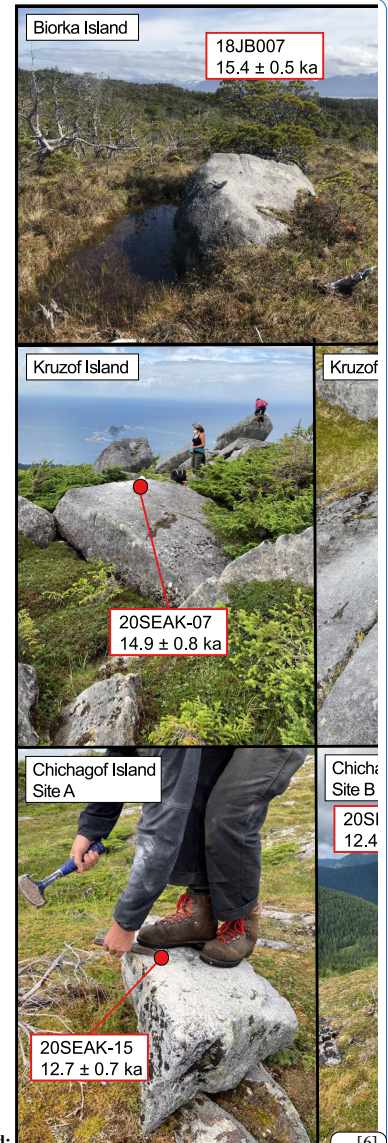
Formatted: Space After: 8 pt, Line spacing: Multiple 1.08 li, Left Horizontal

Formatted

... [5]

Deleted: Note the grooves and chatter marks on bedrock of 19SEAK-18.

Formatted: Font: Times New Roman



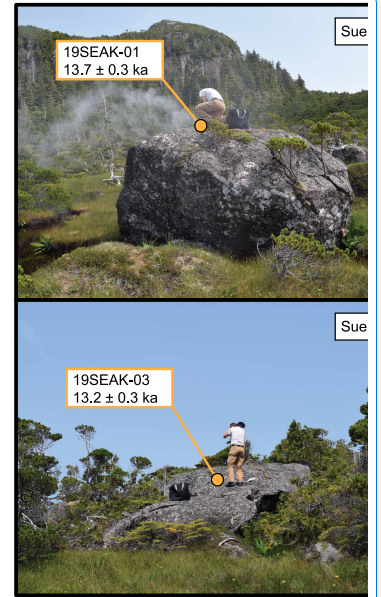
Deleted:

... [6]

1250 **Figure 4:** Sample photos from 2018 and 2020 field season. All ^{10}Be ages are shown with 1σ
 1251 internal uncertainty. Note the relatively small size of 20SEAK-15.



1254
 1255
 1256 **Figure 5:** Basalt samples and ^{36}Cl ages from southwestern Suemez Island. Ages are reported at 1σ
 1257 internal uncertainty.



35

Formatted: Default Paragraph Font, Font: +Body (Calibri), Font color: Black

Formatted: Default Paragraph Font, Font: +Body (Calibri), Font color: Black

Formatted: ... [7]

Formatted: Font: Calibri, Font color: Black

Formatted: Font: Not Bold

Formatted: Space Before: 12 pt, After: 12 pt, Line spacing: Multiple 1.08 li, Left Horizontal

Formatted: Font color: Auto

Formatted: Font color: Auto, Not Superscript/ Subscript

Formatted: Font color: Auto

Formatted: Font: Times New Roman

Deleted:

Formatted: Font color: Auto

Formatted: Space Before: 12 pt, After: 12 pt, Line spacing: Multiple 1.08 li, Left Horizontal

Formatted: Font: Bold, Font color: Auto

Formatted: Font color: Auto

Formatted: Font color: Auto

Deleted: ¶

Formatted: ¶

Formatted: Font: 11 pt, Bold, Font color: Auto

Formatted: Line spacing: Multiple 1.08 li, Left Horizontal

1250
 1251
 1252
 1253

1254
 1255

1256
 1257

1258
 1259

1260
 1261

1262
 1263

1264
 1265

1269
1270
1271
1272
1273

Table 1: ¹⁰Be surface exposure age data

36

Formatted: Default Paragraph Font, Font: +Body (Calibri), Font color: Black

Formatted: Default Paragraph Font, Font: +Body (Calibri), Font color: Black

Formatted: Normal, Right, Border: Top: (No border), Bottom: (No border), Left: (No border), Right: (No border), Between : (No border), Tab stops: 3.25", Centered + 6.5"; Right, Position: Horizontal: Left, Relative to: Column, Vertical: In line, Relative to: Margin, Wrap Around

Formatted: Font: Calibri, Font color: Black

Formatted: Font: 11 pt, Bold, Font color: Auto

Formatted: Line spacing: Multiple 1.08 li, Left Horizontal

Formatted: Font: Bold, Font color: Auto

Formatted: Font color: Auto

Deleted: .

Formatted: Font color: Auto

1275
1276
1277

Table 2: ^{36}Cl surface exposure age data

Sample ID	Sample type	Latitude (°N)	Longitude (°W)	Elevation (m asl)	Sample thickness (cm)	Topographic shielding correction	Quartz (g)	$^{36}\text{Be}/\text{Be}$ ratio ^a	^{36}Be uncertainty (atoms/g)	^{36}Be (atoms/g)	^{36}Th ratio uncertainty	^{36}Th (atoms/g)	^{36}Th uncertainty (atoms/g)	^{36}Th age ^b (years)	^{36}Th age ^c (years)	^{36}Th age ^d (years)
TERRACELAND																
18180A6-1	Boulder	56.8482	-135.5116	47	1.0	1.000	24.17	232	1.30E-15	6.60E-04	1.40E-15	2.12E-05	182.0±0.5 (8.9)	145.0±0.5 (1.2)		
18180A6-2	Boulder	56.8471	-135.5115	47	1.2	1.000	24.27	221	1.32E-15	6.49E-04	4.37E-15	2.25E-05	149.0±0.8 (8.8)	143.0±0.5 (1.2)		
18180B7	Boulder	56.8527	-135.5355	46	1.0	1.000	35.52	235	1.35E-15	6.40E-04	4.56E-15	2.26E-05	174.0±0.5 (8.8)	143.0±0.5 (1.1)		
18180B8	Boulder	56.8528	-135.5362	46	1.0	1.000	24.35	232	1.40E-15	5.90E-04	2.02E-15	1.99E-05	137.0±0.5 (8.7)	143.0±0.5 (1.1)		
SIEMEZ ISLAND																
18180A6-3	Boulder	56.8689	-133.4416	376	2.0	0.958	21.24	233	1.20E-15	6.10E-04	2.42E-15	3.07E-05	176.0±0.7 (8.9)	144.0±0.6 (1.3)		
18180A6-4	Boulder	56.8687	-133.4416	376	2.0	0.958	21.26	233	1.20E-15	6.10E-04	2.42E-15	3.07E-05	176.0±0.7 (8.9)	144.0±0.6 (1.3)		
18180A6-5	Boulder	56.8689	-133.4416	376	2.0	0.958	21.24	233	1.20E-15	6.10E-04	2.42E-15	3.07E-05	176.0±0.7 (8.9)	144.0±0.6 (1.3)		
18180A6-6	Boulder	56.8687	-133.4416	376	2.0	0.958	21.26	233	1.20E-15	6.10E-04	2.42E-15	3.07E-05	176.0±0.7 (8.9)	144.0±0.6 (1.3)		
18180A6-7	Boulder	56.8689	-133.4416	376	2.0	0.958	21.24	233	1.20E-15	6.10E-04	2.42E-15	3.07E-05	176.0±0.7 (8.9)	144.0±0.6 (1.3)		
18180A6-8	Boulder	56.8687	-133.4416	376	2.0	0.958	21.26	233	1.20E-15	6.10E-04	2.42E-15	3.07E-05	176.0±0.7 (8.9)	144.0±0.6 (1.3)		
18180A6-9	Boulder	56.8689	-133.4416	376	2.0	0.958	21.24	233	1.20E-15	6.10E-04	2.42E-15	3.07E-05	176.0±0.7 (8.9)	144.0±0.6 (1.3)		
18180A6-10	Boulder	56.8687	-133.4416	376	2.0	0.958	21.26	233	1.20E-15	6.10E-04	2.42E-15	3.07E-05	176.0±0.7 (8.9)	144.0±0.6 (1.3)		
BARANOV ISLAND																
18180A6-11	Boulder	56.3677	-134.9015	140	2.0	0.923	25.08	233	1.30E-15	6.21E-04	3.24E-15	2.48E-05	163.0±0.8			
18180A6-12	Boulder	56.3677	-134.9015	140	2.0	0.923	25.08	233	1.30E-15	6.21E-04	3.24E-15	2.48E-05	163.0±0.8			
18180A6-13	Boulder	56.3718	-134.9094	126	2.0	1.000	24.80	233	1.31E-15	6.19E-04	5.09E-15	5.09E-05	280.0±1.1	269.1±1.0		
18180A6-14	Boulder	56.3718	-134.9094	126	2.0	1.000	24.80	233	1.31E-15	6.19E-04	5.09E-15	5.09E-05	280.0±1.1	269.1±1.0		
18180A6-15	Boulder	56.3712	-134.9082	135	2.0	1.000	25.03	233	1.09E-15	6.80E-04	3.47E-15	3.47E-05	134.0±0.7	138.0±0.6		
18180A6-16	Boulder	56.3676	-134.9088	48	2.0	1.000	25.06	233	1.08E-15	6.52E-04	2.84E-15	2.84E-05	144.0±0.7	138.0±0.6		
18180A6-17	Boulder	56.3676	-134.9072	48	2.0	0.979	20.17	230	1.03E-15	6.13E-04	2.84E-15	2.84E-05	144.0±0.6	138.0±0.6		
18180A6-18	Boulder	56.3676	-134.9072	48	2.0	0.979	20.17	230	1.03E-15	6.13E-04	2.84E-15	2.84E-05	144.0±0.6	138.0±0.6		
18180A6-19	Boulder	56.3676	-134.9072	48	2.0	0.979	20.17	230	1.03E-15	6.13E-04	2.84E-15	2.84E-05	144.0±0.6	138.0±0.6		
18180A6-20	Boulder	56.3676	-134.9072	48	2.0	0.979	20.17	230	1.03E-15	6.13E-04	2.84E-15	2.84E-05	144.0±0.6	138.0±0.6		
18180A6-21	Boulder	56.3676	-134.9072	48	2.0	0.979	20.17	230	1.03E-15	6.13E-04	2.84E-15	2.84E-05	144.0±0.6	138.0±0.6		
18180A6-22	Boulder	56.3676	-134.9072	48	2.0	0.979	20.17	230	1.03E-15	6.13E-04	2.84E-15	2.84E-05	144.0±0.6	138.0±0.6		
18180A6-23	Boulder	56.3676	-134.9072	48	2.0	0.979	20.17	230	1.03E-15	6.13E-04	2.84E-15	2.84E-05	144.0±0.6	138.0±0.6		
18180A6-24	Boulder	56.3676	-134.9072	48	2.0	0.979	20.17	230	1.03E-15	6.13E-04	2.84E-15	2.84E-05	144.0±0.6	138.0±0.6		
18180A6-25	Boulder	56.3676	-134.9072	48	2.0	0.979	20.17	230	1.03E-15	6.13E-04	2.84E-15	2.84E-05	144.0±0.6	138.0±0.6		
18180A6-26	Boulder	56.3676	-134.9072	48	2.0	0.979	20.17	230	1.03E-15	6.13E-04	2.84E-15	2.84E-05	144.0±0.6	138.0±0.6		
18180A6-27	Boulder	56.3676	-134.9072	48	2.0	0.979	20.17	230	1.03E-15	6.13E-04	2.84E-15	2.84E-05	144.0±0.6	138.0±0.6		
18180A6-28	Boulder	56.3676	-134.9072	48	2.0	0.979	20.17	230	1.03E-15	6.13E-04	2.84E-15	2.84E-05	144.0±0.6	138.0±0.6		
18180A6-29	Boulder	56.3676	-134.9072	48	2.0	0.979	20.17	230	1.03E-15	6.13E-04	2.84E-15	2.84E-05	144.0±0.6	138.0±0.6		
18180A6-30	Boulder	56.3676	-134.9072	48	2.0	0.979	20.17	230	1.03E-15	6.13E-04	2.84E-15	2.84E-05	144.0±0.6	138.0±0.6		
CHIYOGAI ISLAND																
20518A6-1	Boulder	57.4621	-135.6554	476	0.5	1.000	20.25	230	1.34E-15	6.46E-15	1.01E-15	4.80E-05	153.0±0.7 (8.9)	144.0±0.7 (1.3)		
20518A6-2	Boulder	57.4621	-135.6554	476	0.5	1.000	20.25	230	1.34E-15	6.46E-15	1.01E-15	4.80E-05	153.0±0.7 (8.9)	144.0±0.7 (1.3)		
20518A6-3	Boulder	57.4621	-135.6554	476	0.5	1.000	20.25	230	1.34E-15	6.46E-15	1.01E-15	4.80E-05	153.0±0.7 (8.9)	144.0±0.7 (1.3)		
20518A6-4	Boulder	57.4621	-135.6554	476	0.5	1.000	20.25	230	1.34E-15	6.46E-15	1.01E-15	4.80E-05	153.0±0.7 (8.9)	144.0±0.7 (1.3)		
20518A6-5	Boulder	57.4621	-135.6554	476	0.5	1.000	20.25	230	1.34E-15	6.46E-15	1.01E-15	4.80E-05	153.0±0.7 (8.9)	144.0±0.7 (1.3)		
20518A6-6	Boulder	57.4621	-135.6554	476	0.5	1.000	20.25	230	1.34E-15	6.46E-15	1.01E-15	4.80E-05	153.0±0.7 (8.9)	144.0±0.7 (1.3)		
20518A6-7	Boulder	57.4621	-135.6554	476	0.5	1.000	20.25	230	1.34E-15	6.46E-15	1.01E-15	4.80E-05	153.0±0.7 (8.9)	144.0±0.7 (1.3)		
20518A6-8	Boulder	57.4621	-135.6554	476	0.5	1.000	20.25	230	1.34E-15	6.46E-15	1.01E-15	4.80E-05	153.0±0.7 (8.9)	144.0±0.7 (1.3)		
20518A6-9	Boulder	57.4621	-135.6554	476	0.5	1.000	20.25	230	1.34E-15	6.46E-15	1.01E-15	4.80E-05	153.0±0.7 (8.9)	144.0±0.7 (1.3)		
20518A6-10	Boulder	57.4621	-135.6554	476	0.5	1.000	20.25	230	1.34E-15	6.46E-15	1.01E-15	4.80E-05	153.0±0.7 (8.9)	144.0±0.7 (1.3)		
20518A6-11	Boulder	57.4621	-135.6554	476	0.5	1.000	20.25	230	1.34E-15	6.46E-15	1.01E-15	4.80E-05	153.0±0.7 (8.9)	144.0±0.7 (1.3)		
20518A6-12	Boulder	57.4621	-135.6554	476	0.5	1.000	20.25	230	1.34E-15	6.46E-15	1.01E-15	4.80E-05	153.0±0.7 (8.9)	144.0±0.7 (1.3)		
20518A6-13	Boulder	57.4621	-135.6554	476	0.5	1.000	20.25	230	1.34E-15	6.46E-15	1.01E-15	4.80E-05	153.0±0.7 (8.9)	144.0±0.7 (1.3)		
20518A6-14	Boulder	57.4621	-135.6554	476	0.5	1.000	20.25	230	1.34E-15	6.46E-15	1.01E-15	4.80E-05	153.0±0.7 (8.9)	144.0±0.7 (1.3)		
20518A6-15	Boulder	57.4621	-135.6554	476	0.5	1.000	20.25	230	1.34E-15	6.46E-15	1.01E-15	4.80E-05	153.0±0.7 (8.9)	144.0±0.7 (1.3)		
20518A6-16	Boulder	57.4621	-135.6554	476	0.5	1.000	20.25	230	1.34E-15	6.46E-15	1.01E-15	4.80E-05	153.0±0.7 (8.9)	144.0±0.7 (1.3)		
20518A6-17	Boulder	57.4621	-135.6554	476	0.5	1.000	20.25	230	1.34E-15	6.46E-15	1.01E-15	4.80E-05	153.0±0.7 (8.9)	144.0±0.7 (1.3)		
20518A6-18	Boulder	57.4621	-135.6554	476	0.5	1.000	20.25	230	1.34E-15	6.46E-15	1.01E-15	4.80E-05	153.0±0.7 (8.9)	144.0±0.7 (1.3)		
20518A6-19	Boulder	57.4621	-135.6554	476	0.5	1.000	20.25	230	1.34E-15	6.46E-15	1.01E-15	4.80E-05	153.0±0.7 (8.9)	144.0±0.7 (1.3)		
20518A6-20	Boulder	57.4621	-135.6554	476	0.5	1.000	20.25	230	1.34E-15	6.46E-15	1.01E-15	4.80E-05	153.0±0.7 (8.9)	144.0±0.7 (1.3)		
20518A6-21	Boulder	57.4621	-135.6554	476	0.5	1.000	20.25	230	1.34E-15	6.46E-15	1.01E-15	4.80E-05	153.0±0.7 (8.9)	144.0±0.7 (1.3)		
20518A6-22	Boulder	57.4621	-135.6554	476	0.5	1.000	20.25	230	1.34E-15	6.46E-15	1.01E-15	4.80E-05	153.0±0.7 (8.9)	144.0±0.7 (1.3)		

^aThe $^{36}\text{Be}/\text{Be}$ ratio was measured with a Cameca IMS-127 ion microprobe (5–5 cm vertical uncertainty) at UCLA. ^{36}Be is in atoms per gram. ^b ^{36}Th is in atoms per gram. ^cAge is in years. ^dAge is in years. ^eAge is in years. ^fAge is in years. ^gAge is in years. ^hAge is in years. ⁱAge is in years. ^jAge is in years. ^kAge is in years. ^lAge is in years. ^mAge is in years. ⁿAge is in years. ^oAge is in years. ^pAge is in years. ^qAge is in years. ^rAge is in years. ^sAge is in years. ^tAge is in years. ^uAge is in years. ^vAge is in years. ^wAge is in years. ^xAge is in years. ^yAge is in years. ^zAge is in years. ^{aa}Age is in years. ^{ab}Age is in years. ^{ac}Age is in years. ^{ad}Age is in years. ^{ae}Age is in years. ^{af}Age is in years. ^{ag}Age is in years. ^{ah}Age is in years. ^{ai}Age is in years. ^{aj}Age is in years. ^{ak}Age is in years. ^{al}Age is in years. ^{am}Age is in years. ^{an}Age is in years. ^{ao}Age is in years. ^{ap}Age is in years. ^{aq}Age is in years. ^{ar}Age is in years. ^{as}Age is in years. ^{at}Age is in years. ^{au}Age is in years. ^{av}Age is in years. ^{aw}Age is in years. ^{ax}Age is in years. ^{ay}Age is in years. ^{az}Age is in years. ^{ba}Age is in years. ^{bb}Age is in years. ^{bc}Age is in years. ^{bd}Age is in years. ^{be}Age is in years. ^{bf}Age is in years. ^{bg}Age is in years. ^{bh}Age is in years. ^{bi}Age is in years. ^{bj}Age is in years. ^{bk}Age is in years. ^{bl}Age is in years. ^{bm}Age is in years. ^{bn}Age is in years. ^{bo}Age is in years. ^{bp}Age is in years. ^{bq}Age is in years. ^{br}Age is in years. ^{bs}Age is in years. ^{bt}Age is in years. ^{bu}Age is in years. ^{bv}Age is in years. ^{bw}Age is in years. ^{bx}Age is in years. ^{by}Age is in years. ^{bz}Age is in years. ^{ca}Age is in years. ^{cb}Age is in years. ^{cc}Age is in years. ^{cd}Age is in years. ^{ce}Age is in years. ^{cf}Age is in years. ^{cg}Age is in years. ^{ch}Age is in years. ^{ci}Age is in years. ^{cj}Age is in years. ^{ck}Age is in years. ^{cl}Age is in years. ^{cm}Age is in years. ^{cn}Age is in years. ^{co}Age is in years. ^{cp}Age is in years. ^{cq}Age is in years. ^{cr}Age is in years. ^{cs}Age is in years. ^{ct}Age is in years. ^{cu}Age is in years. ^{cv}Age is in years. ^{cw}Age is in years. ^{cx}Age is in years. ^{cy}Age is in years. ^{cz}Age is in years. ^{da}Age is in years. ^{db}Age is in years. ^{dc}Age is in years. ^{dd}Age is in years. ^{de}Age is in years. ^{df}Age is in years. ^{dg}Age is in years. ^{dh}Age is in years. ^{di}Age is in years. ^{dj}Age is in years. ^{dk}Age is in years. ^{dl}Age is in years. ^{dm}Age is in years. ^{dn}Age is in years. ^{do}Age is in years. ^{dp}Age is in years. ^{dq}Age is in years. ^{dr}Age is in years. ^{ds}Age is in years. ^{dt}Age is in years. ^{du}Age is in years. ^{dv}Age is in years. ^{dw}Age is in years. ^{dx}Age is in years. ^{dy}Age is in years. ^{dz}Age is in years. ^{ea}Age is in years. ^{eb}Age is in years. ^{ec}Age is in years. ^{ed}Age is in years. ^{ee}Age is in years. ^{ef}Age is in years. ^{eg}Age is in years. ^{eh}Age is

Sample ID	Sample type	Latitude (°N)	Longitude (°W)	Elevation (masl) ^a	Sample thickness (cm)	Density (g/cm ³)	Topographic Shielding Correction	Aliquot mass of 37Cl-enriched spike (μg)	37Cl-enriched spike to natural 37Cl ratio (atoms/g)	37Cl/37Cl ⁿ ratio (ppm)	Total Cl concentration (μg/g)	Rock composition (μg/g)	Natural 37Cl concentration (μg/g)	36Cl/37Cl ratio (atoms/g)	36Cl concentration (atoms/g)	36Cl uncertainty (atoms/g)	36Cl age (ka)	36Cl age uncertainty (ka)	
ROCK SAMPLES																			
198AK-01	Boulder	55.2449	-133.4328	391	2.5	2.8	0.99858	1.205	78.4	1.18	12.9 ± 0.8	12.914	0.249	1.47E-15	3.76E-15	2.41E-03	13.3 ± 0.3 (1.3)		
198AK-02	Boulder	55.2461	-133.4327	398	2.5	2.8	0.99866	1.833	78.2	1.32E-13	3.7 ± 0.1	11.581	0.327	1.24E-15	3.87E-15	3.73E-03	16.4 ± 0.5 (1.3)		
198AK-03	Boulder	55.246	-133.4324	398	2.5	2.8	0.99866	1.201	78.5	1.03E-13	24.0 ± 0.8	14.008	0.119	2.80E-15	4.38E-15	2.07E-03	13.1 ± 0.3 (1.3)		
198AK-06	Boulder	55.2448	-133.4335	398	2	2.8	0.998524	1.201	78.5	6.02E-14	3.3 ± 0.5	20.259	0.219	2.43E-15	3.01E-15	2.19E-03	12.4 ± 0.3 (1.3)		
CLBK-A04	-	-	-	-	-	-	-	-	78.0	-	-	-	-	-	-	-	-	-	
CLBK-A08	-	-	-	-	-	-	-	-	78.0	-	-	-	-	-	-	-	-	-	
CLBK-26	-	-	-	-	-	-	-	-	78.6	-	-	-	-	-	-	-	-	-	

^a The 37Cl-enriched spike was made at Lawrence Livermore National Laboratory. Its Cl concentration is 1285 ppm and its 35Cl/37Cl ratio is 0.93.
^b The natural Cl carrier was made at the University of New Hampshire. Its Cl concentration is 1436 ± 9 ppm and its 35Cl/37Cl ratio is 3.127.
^c Uncertainties on 35Cl/37Cl and 36Cl/37Cl ratios and exposure ages represent propagated 1-σ analytical uncertainties only.
^d Sample 36Cl concentrations were corrected for 36S using the CRONUS36 correction factors (https://www.earth.berkeley.edu/~dave/cronus36.html).
^e Exposure ages are presented at 1-σ internal uncertainty. Ages were calculated with the CRONUS36 36Cl calibration (https://www.earth.berkeley.edu/~dave/cronus36.html) and an scaling factor of 1.0.
^f Aliquot for stable Cl concentration presented with CLBK-A04.
^g Aliquot for 36Cl concentration presented with CLBK-A04.
^h Aliquot for stable Cl concentration presented with CLBK-A04.

Formatted: Default Paragraph Font, Font: +Body (Calibri), Font color: Black

Formatted: Normal, Right, Border: Top: (No border), Bottom: (No border), Left: (No border), Right: (No border), Between : (No border), Tab stops: 3.25", Centered + 6.5", Right, Position: Horizontal: Left, Relative to: Column, Vertical: In line, Relative to: Margin, Wrap Around

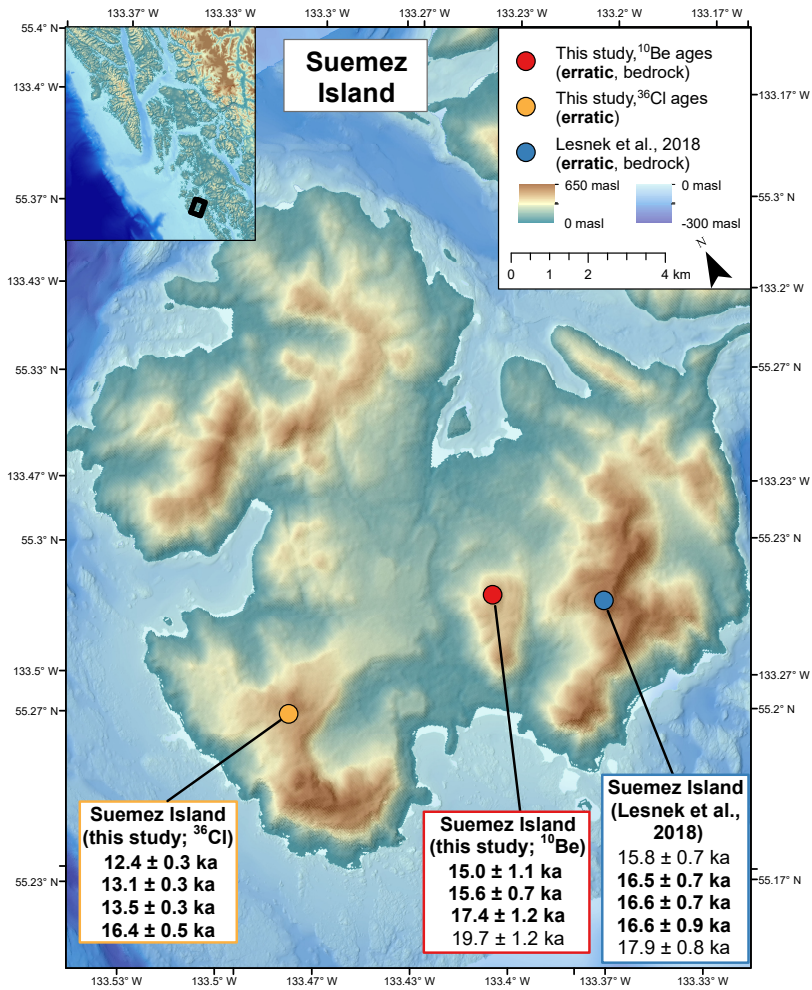
Formatted: Default Paragraph Font, Font: +Body (Calibri), Font color: Black

Formatted: Font: Calibri, Font color: Black

Sample ID	Sample type	Latitude (°N)	Longitude (°W)	Elevation (masl) ^a	Sample thickness (cm)	Density (g/cm ³)	Topographic Shielding Correction	Aliquot mass of 37Cl-enriched spike (μg)	37Cl-enriched spike to natural 37Cl ratio (atoms/g)	37Cl/37Cl ⁿ ratio (ppm)	Total Cl concentration (μg/g)	Rock composition (μg/g)	Natural 37Cl concentration (μg/g)	36Cl/37Cl ratio (atoms/g)	36Cl concentration (atoms/g)	36Cl uncertainty (atoms/g)	36Cl age (ka)	36Cl age uncertainty (ka)	
ROCK SAMPLES																			
198AK-01	Boulder	55.2449	-133.4328	391	2.5	2.8	0.99858	1.184	0.087	1.36E-13	12.014	12.014	0.249	1.50E-13	3.34E-15	2.33E-03	13.7 ± 0.3		
198AK-02	Boulder	55.2461	-133.4327	398	2.5	2.8	0.99866	1.033	0.093	1.32E-13	11.581	11.581	0.327	1.77E-13	5.07E-15	3.69E-03	16.6 ± 0.5		
198AK-03	Boulder	55.246	-133.4324	398	2.5	2.8	0.99866	1.201	0.095	1.35E-13	14.008	14.008	0.119	2.02E-13	4.30E-15	2.61E-03	13.2 ± 0.3		
198AK-06	Boulder	55.2448	-133.4335	398	2	2.8	0.998524	1.201	0.0619	8.01E-14	20.0269	20.0269	0.219	2.46E-13	5.43E-15	2.29E-03	12.5 ± 0.3		
CLBK-A04	-	-	-	-	-	-	-	0.0607	0.953	-	-	-	-	-	-	-	-	-	
CLBK-A08	-	-	-	-	-	-	-	0.0596	0.926	-	-	-	-	-	-	-	-	-	
CLBK-26	-	-	-	-	-	-	-	0.0607	0.953	-	-	-	-	-	-	-	-	-	

^a The 37Cl-enriched spike was made at Lawrence Livermore National Laboratory. Its Cl concentration is 1285 ppm and its 35Cl/37Cl ratio is 0.93.
^b The natural Cl carrier was made at the University of New Hampshire. Its Cl concentration is 1436 ± 9 ppm and its 35Cl/37Cl ratio is 3.127.
^c Uncertainties on 35Cl/37Cl and 36Cl/37Cl ratios and exposure ages represent propagated 1-σ analytical uncertainties only.
^d Sample 36Cl concentrations were corrected for 36S using the CRONUS36 correction factors (https://www.earth.berkeley.edu/~dave/cronus36.html) and an scaling factor of 1.0.
^e Exposure ages are presented at 1-σ internal uncertainty. Ages were calculated with the CRONUS36 36Cl calibration (https://www.earth.berkeley.edu/~dave/cronus36.html) and an scaling factor of 1.0.
^f Aliquot for stable Cl concentration presented with CLBK-A04.
^g Aliquot for 36Cl concentration presented with CLBK-A04.

Deleted:



39

Formatted: Default Paragraph Font, Font: +Body (Calibri), Font color: Black

Formatted: Normal, Right, Border: Top: (No border), Bottom: (No border), Left: (No border), Right: (No border), Between: (No border), Tab stops: 3.25", Centered + 6.5", Right, Position: Horizontal: Left, Relative to: Column, Vertical: In line, Relative to: Margin, Wrap Around

Formatted: Default Paragraph Font, Font: +Body (Calibri), Font color: Black

Formatted: Font: Calibri, Font color: Black

1287

1288

1289 Figure 6: ¹⁰Be and ³⁶Cl ages from samples collected on Suemez on island: red and yellow dots
 1290 mark sampling site from this study, blue dot marks sampling site from Lesnek et al. (2018). Bold
 1291 ages are from boulders; plain ages are from bedrock. All ¹⁰Be and ³⁶Cl ages reported with 1 σ
 1292 internal uncertainty.

Formatted: Font color: Auto

Formatted: Space Before: 12 pt, After: 12 pt, Line spacing: Multiple 1.08 li, Left Horizontal

Deleted: dot marks

Formatted: Font color: Auto

Deleted: ,

Formatted: Font color: Auto

Formatted: Font color: Auto

Formatted: Font: Times New Roman

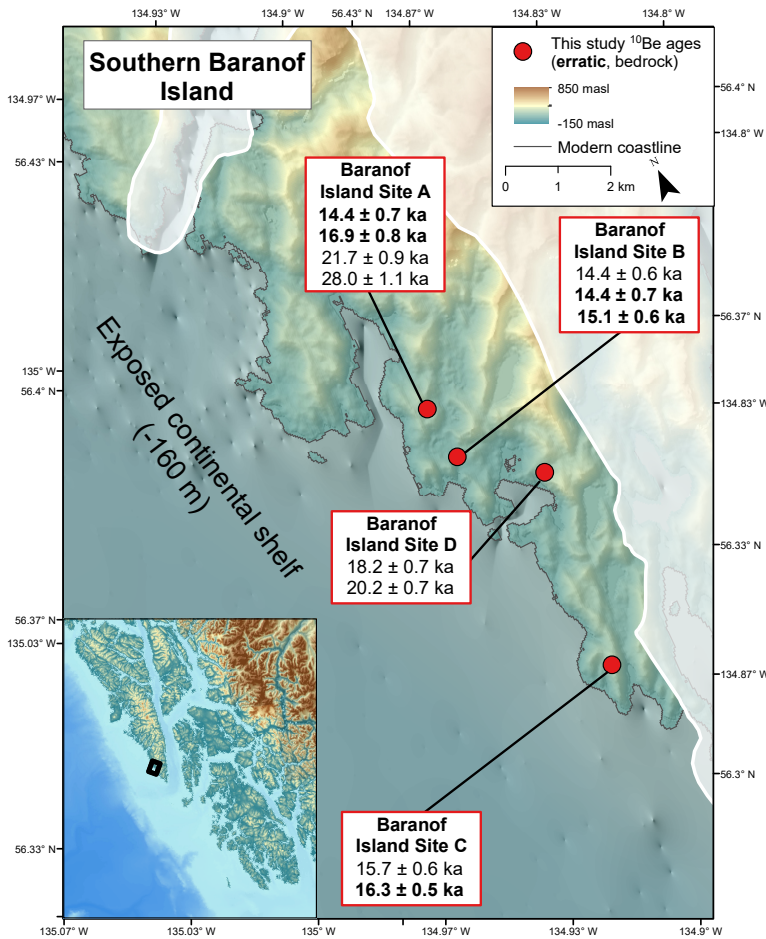


Figure 7: ¹⁰Be ages from sampling sites on southern Baranof Island. **Bold ages are from boulders; plain ages are from bedrock.** All ages are reported with 1 σ internal error. Cordilleran Ice Sheet LIGM extent after Carrara et al. (2007).

40

Formatted: Default Paragraph Font, Font: +Body (Calibri), Font color: Black

Formatted: Default Paragraph Font, Font: +Body (Calibri), Font color: Black

Formatted: Normal, Right, Border: Top: (No border), Bottom: (No border), Left: (No border), Right: (No border), Between: (No border), Tab stops: 3.25", Centered + 6.5", Right, Position: Horizontal: Left, Relative to: Column, Vertical: In line, Relative to: Margin, Wrap Around

Formatted: Font: Calibri, Font color: Black

Deleted: [1]

Formatted: Font color: Auto

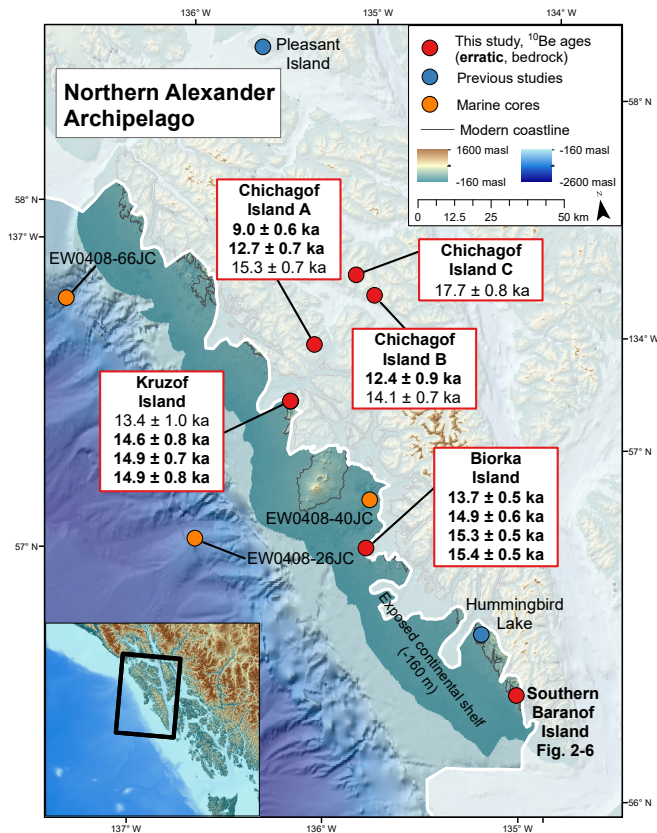
Formatted: Space Before: 12 pt, After: 12 pt, Line spacing: Multiple 1.08 li, Left Horizontal

Formatted: Font color: Auto

Deleted: CIS ILGM

Formatted: Font color: Auto

Formatted: Font: Times New Roman



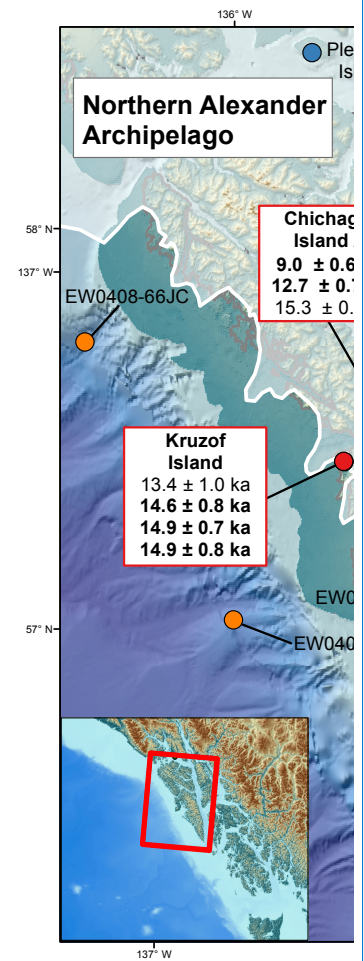
41

Formatted: Normal, Right, Border: Top: (No border), Bottom: (No border), Left: (No border), Right: (No border), Between: (No border), Tab stops: 3.25", Centered + 6.5", Right, Position: Horizontal: Left, Relative to: Column, Vertical: In line, Relative to: Margin, Wrap Around

Formatted: Default Paragraph Font, Font: +Body (Calibri), Font color: Black

Formatted: Default Paragraph Font, Font: +Body (Calibri), Font color: Black

Formatted: Font: Calibri, Font color: Black



Deleted:

Formatted: Font color: Auto

Formatted: Space After: 8 pt, Line spacing: Multiple 1.08 li, Left Horizontal

Deleted: ILGM CIS

Formatted

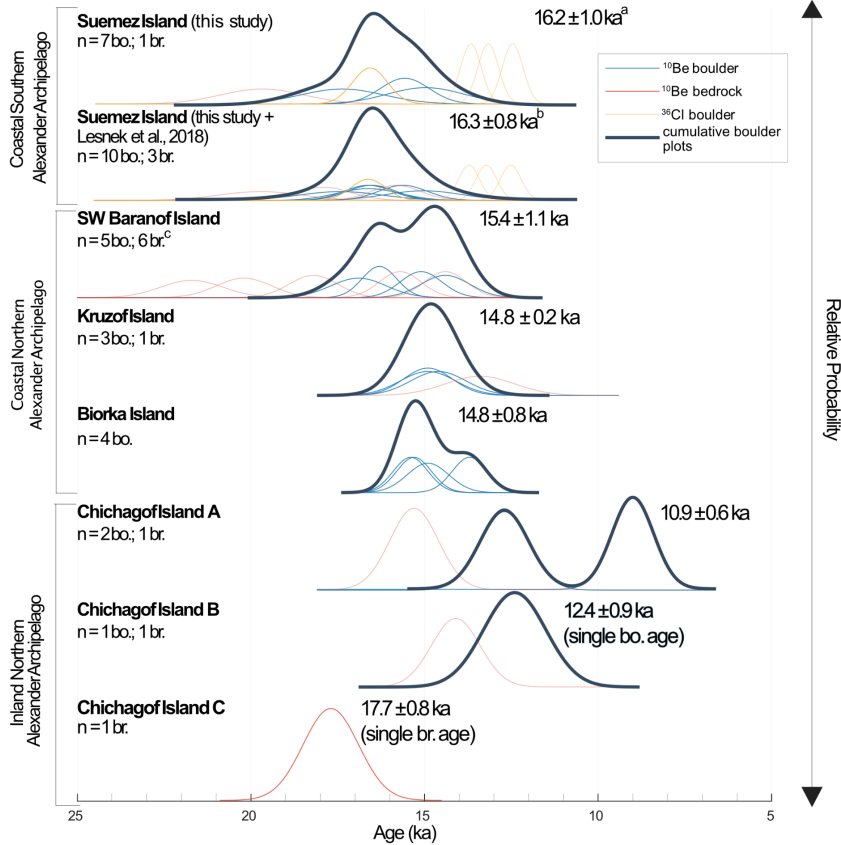
[12]

1306

1307

1308

1309 Figure 8: ^{10}Be ages from sampling sites in the northern Alexander Archipelago. All ages are
 1310 reported with 1σ internal error. **Bold ages are from boulders; plain ages are from bedrock.**
 1311 **LLGM Cordilleran Ice Sheet** extent after Lesnek et al. (2020). Exposed continental shelf at -160
 1312 m below modern sea level Baichtal et al. (in press). Yellow dots show location of relevant
 1313 marine sediment cores: EW0408-66JC and EW0408-26JC (Praetorius and Mix, 2014; Praetorius
 1314 et al., 2016) and EW0408-40JC (Addison et al., 2010). Blue dots show locations of relevant
 1315 terrestrial study sites: Pleasant Island (Hansen and Engstrom, 1996) and Hummingbird Lake
 1316 (Ager, 2019).

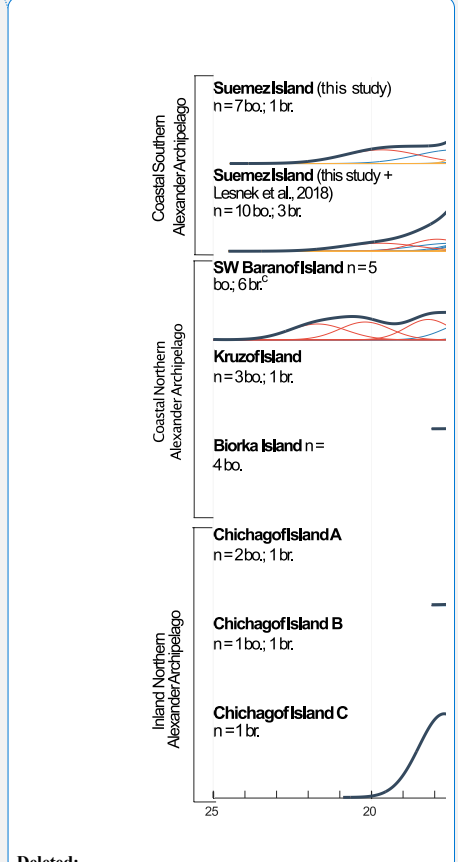


Formatted: Default Paragraph Font, Font: +Body (Calibri), Font color: Black

Formatted: Default Paragraph Font, Font: +Body (Calibri), Font color: Black

Formatted: Normal, Right, Border: Top: (No border), Bottom: (No border), Left: (No border), Right: (No border), Between : (No border), Tab stops: 3.25", Centered + 6.5", Right, Position: Horizontal: Left, Relative to: Column, Vertical: In line, Relative to: Margin, Wrap Around

Formatted: Font: Calibri, Font color: Black



Deleted:

Formatted: Font color: Auto

Formatted: Space After: 8 pt, Line spacing: Multiple 1.08 li, Left Horizontal

Formatted: Font color: Auto

Formatted: Font: Times New Roman

Deleted: ¶

¶

¶

¶

1321

1322

1323

1324

1325

1326

1327

1328

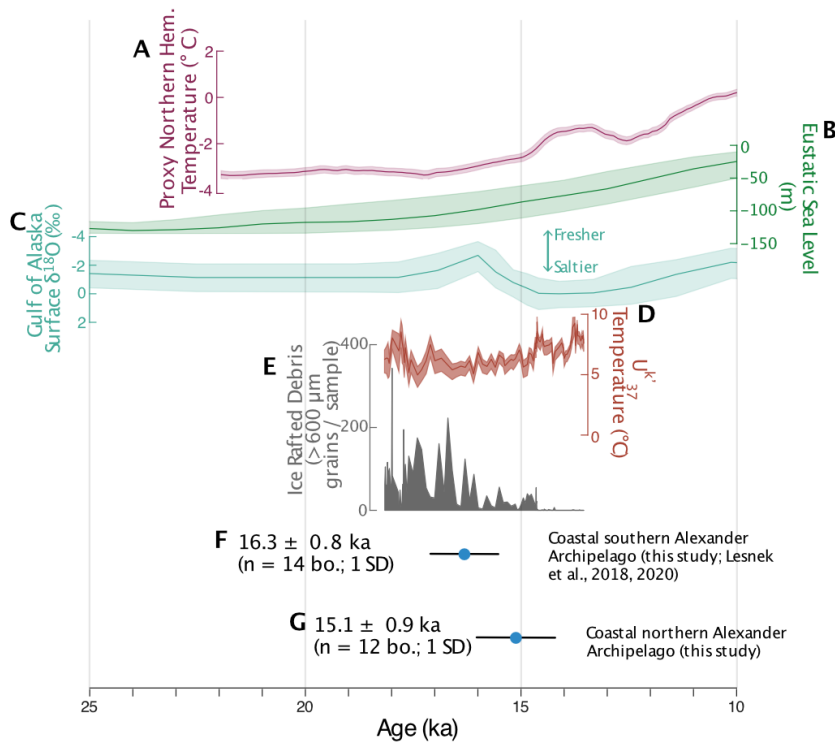
1329

1330

1331

Figure 9: Relative probably plots of bedrock (red) and boulder (blue) ¹⁰Be and ³⁶Cl boulder (yellow) ages from this study calculated with 1 σ internal uncertainty. bo. = boulder, br. = bedrock. All ages shown are mean ages from only boulders at each sample site reported with 1 SD unless noted. Cumulative plots represent all bold lines - transparent lines were not included in their calculation. ^aAverage of all ¹⁰Be boulder ages and oldest ³⁶Cl boulder age with 1 SD. ^bAverage of all ¹⁰Be boulder ages (this study and Lesnek et al., 2018) and oldest ³⁶Cl boulder age (this study). ^cOne old outlier at 28.0 ± 1.1 ka not shown.

1342



43

Formatted: Normal, Right, Border: Top: (No border), Bottom: (No border), Left: (No border), Right: (No border), Between: (No border), Tab stops: 3.25", Centered + 6.5", Right, Position: Horizontal: Left, Relative to: Column, Vertical: In line, Relative to: Margin, Wrap Around

Formatted: Default Paragraph Font, Font: +Body (Calibri), Font color: Black

Formatted: Default Paragraph Font, Font: +Body (Calibri), Font color: Black

Formatted: Font: Calibri, Font color: Black

1343

1344

1345

1346 Figure 10: A) Proxy Northern Hemisphere temperature anomaly relative to early Holocene with
 1347 1σ error (Shakun et al., 2012). B) Eustatic sea-level curve (Spratt and Lisiecki, 2016). C) Gulf of
 1348 Alaska surface salinity $\delta^{18}O$ record (Core SO202-27-6; Maier et al., 2018). D) U^k_{37}
 1349 temperature reconstruction from off the coast of the Alexander Archipelago (Cores EW0408-
 1350 26JC, EW0408-66JC; Praetorius et al., 2016). E) Ice rafted debris record from off Vancouver
 1351 Island (Core MD02-2496; Cosma et al., 2008). F) & G) Mean boulder ^{10}Be ages from the coastal
 1352 Alexander Archipelago, with 1σ (this study; Lesnek et al., 2018; 2020).

1353

1354

Formatted: Font color: Auto

Formatted: Space After: 8 pt, Line spacing: Multiple 1.08 li, Left Horizontal

Formatted: Font color: Auto, Not Superscript/ Subscript

Formatted: Font color: Auto

Formatted: Font color: Auto, Not Superscript/ Subscript

Formatted: Font color: Auto

Formatted: Font color: Auto

Deleted: -

Formatted: Font color: Auto

Deleted: Relative probability plots of boulder

Formatted: Font color: Auto

Deleted: mean boulder ages and 1σ reported

Formatted: Font color: Auto

Formatted: Font: Times New Roman, 12 pt

1358
1359
1360
1361
1362
1363
1364
1365
1366

44

Formatted: Default Paragraph Font, Font: +Body (Calibri), Font color: Black

Formatted: Normal, Right, Border: Top: (No border), Bottom: (No border), Left: (No border), Right: (No border), Between : (No border), Tab stops: 3.25", Centered + 6.5", Right, Position: Horizontal: Left, Relative to: Column, Vertical: In line, Relative to: Margin, Wrap Around

Formatted: Default Paragraph Font, Font: +Body (Calibri), Font color: Black

Formatted: Font: Calibri, Font color: Black

Formatted: Left

Page 5: [1] Deleted Caleb Walcott 3/11/22 9:09:00 AM



Page 31: [2] Deleted Caleb Walcott 3/11/22 9:09:00 AM



Page 32: [3] Deleted Caleb Walcott 3/11/22 9:11:00 AM



Page 33: [4] Formatted Caleb Walcott 3/11/22 9:09:00 AM

Font color: Auto



Page 33: [4] Formatted Caleb Walcott 3/11/22 9:09:00 AM

Font color: Auto



Page 34: [5] Formatted Caleb Walcott 3/11/22 9:09:00 AM

Font: Bold, Font color: Auto



Page 34: [5] Formatted Caleb Walcott 3/11/22 9:09:00 AM

Font: Bold, Font color: Auto



Page 34: [6] Deleted Caleb Walcott 3/11/22 9:09:00 AM



Page 1: [7] Formatted Caleb Walcott 3/11/22 9:09:00 AM

Normal, Right, Border: Top: (No border), Bottom: (No border), Left: (No border), Right: (No border),
Between : (No border), Tab stops: 3.25", Centered + 6.5", Right, Position: Horizontal: Left, Relative to:
Column, Vertical: In line, Relative to: Margin



Page 37: [8] Deleted Caleb Walcott 3/11/22 9:09:00 AM



Page 37: [9] Formatted Caleb Walcott 3/11/22 9:21:00 AM

Font: Not Bold



Page 37: [9] Formatted Caleb Walcott 3/11/22 9:21:00 AM

Font: Not Bold



Page 38: [10] Deleted **Caleb Walcott** **3/11/22 9:09:00 AM**

x.....

Page 40: [11] Deleted **Caleb Walcott** **3/11/22 9:09:00 AM**

x.....

Page 41: [12] Formatted **Caleb Walcott** **3/11/22 9:09:00 AM**

Font color: Auto ←.....

▲.....

Page 41: [12] Formatted **Caleb Walcott** **3/11/22 9:09:00 AM**

Font color: Auto ←.....

▲.....

Page 42: [13] Deleted **Caleb Walcott** **3/11/22 9:09:00 AM**

x.....